(a)

(b)

Fig. 2. The coated RF antenna inside the discharge chamber of the multicusp field ion source: (a) no RF power; (b) with 120 W RF input and oxygen gas.

function of RF power. It can be seen that the output current increases linearly with RF power. At 500 W RF input, the ion-current densities for argon and helium are 29 and 27 mA $cm^{-2}$, respectively. The reason for obtaining a higher argon current than that of helium is probably due to the fact that argon has a lower ionization potential (15.75 eV) than helium (24.58 eV).

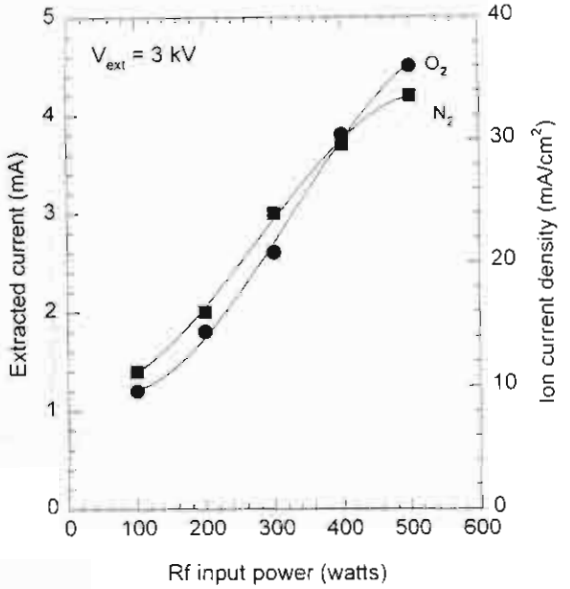


Fig. 4. Extracted ion current and current density versus RF input power for nitrogen and oxygen gases; the extracting voltage is 3 kV operating at a gas pressure of 3 mtorr.

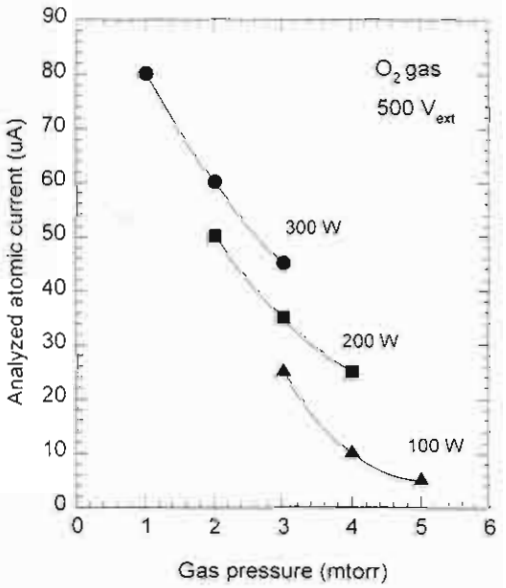


Fig. 5. The relationship between atomic current and gas pressure at different RF powers for oxygen gas.

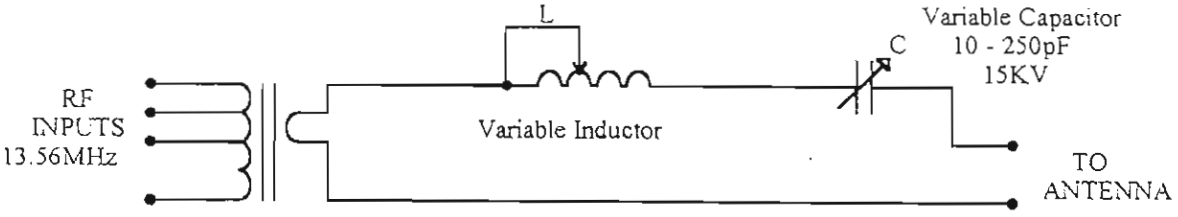


Fig. 3. The isolating and matching circuit for maximum RF power transfer to the multicusp field plasma chamber.

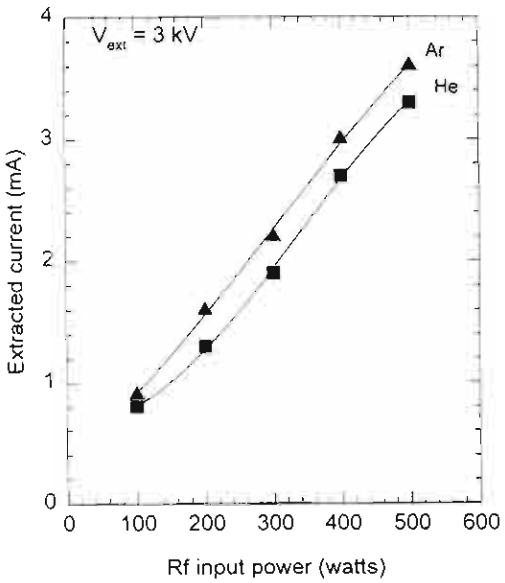


Fig. 6. Extracted ion current versus RF input power for helium and argon gases; the extracting voltage is 3 kV operating at a gas pressure of 10 mtorr.

## 4. Conclusions

We have constructed a 10 cm diameter by 9 cm long RF discharge multicusp ion source operating at 13.56 MHz. Test runs with nitrogen, oxygen, helium and argon gases indicate that the use of a multicusp field makes it possible to attain a higher discharge efficiency at low RF power [8], which should be adequate to operate an ion source for secondary-ion mass spectrometry applications using argon and oxygen gases. Also, the utilization of a high-frequency field makes it possible to operate the source at low pressure. We plan to continue performing experiments with higher RF power inputs up to 3 kW using oxygen and nitrogen for applications in SIMOX (separation by implanted oxygen) and surface modifications of materials.

## Acknowledgements

We would like to thank K.N. Leung of the Lawrence Berkeley National Laboratory for his advice on the design and construction of the ion source. We thank G. DeVries for his help in the construction of an isolation and matching system and B. Saelao for running the MAGNUS program. This work was supported by the National Electronics and Computer Technology Center and the Thai Research Fund.

## References

[1] K.N. Leung, D.A. Bachman, P.R. Herz, D.S. McDonald, Nucl. Instr. Methods B74 (1993) 291.
[2] L.T. Perkin, G.J. DeVries, P.R. Herz, W.B. Kunkel, K.N. Leung, D.S. Pickard, A. Wengrow, M.D. Williams, Rev. Sci. Instrum. 67 (1996) 1.
[3] L.T. Perkin, C. Celata, Y. Lee, K.N. Leung, D.S. Picard, R. Vilaithong, M.D. Williams, D. Wutte, in: J.L. Duggan, I.L. Morgan (Eds.), Proc. of Application of Accelerators in Research and Industry, AIP Press, New York, 1997.
[4] R. Limpaecher, K.R. MacKenzie, Rev. Sci. Instrum. 44 (1973) 726.
[5] T. Shibuya, S. Hashimo, E. Yabe, K. Talkayama, Nucl. Instr. Methods B55 (1991) 364.
[6] MAGNUS, A Three-Dimensional Non-Linear Magnetostatic, Computer Program, supplied by Ferrari Associates, Inc., FL, 1987.
[7] K.L. Ehlers, K.N. Leung, M.D. Williams, Rev. Sci. Instrum. 50 (1979) 1031.
[8] S.R. Walther, K.N. Leung, Vacuum 36 (1986) 869.

# Instructions for Authors

## Submission of Papers

Manuscripts (original and two clear copies) should be submitted to one of the Editors:

for authors in the Americas

**Dr. B. D. Sartwell,** Surface Chemistry Branch, Naval Research Laboratory, Code 6170, Washington, DC 20375, USA;

and for authors elsewhere

**Professor A. Matthews,** Director, The Research Centre in Surface Engineering, The University of Hull, Cottingham Road, North Humberside, HU6 7RX, UK.

Contributions are accepted on the understanding that the authors have obtained the necessary authority for publication. Submission of a manuscript implies that it is not under consideration for publication elsewhere.

## Types of contributions

— original papers
— invited or contributed reviews on specific topics
— brief communications on topics of immediate interest
— notices of meetings, symposia and short courses
— technical notes for "Current Industrial Practices" section

## Languages

Papers will be published in English. Both English and US spelling are permitted, provided that spelling is consistent within an article.

Authors in Japan please note that information about how to have the English of your paper checked, corrected and improved (*before submission*) is available from: Elsevier Science K.K., Editorial Service, 1-9-15 Higashi Azabu, Minato-ku, Tokyo 106-0044, Japan; Tel.: +81 3 5561 5032; Fax: +81 3 5561 5045.

## Manuscript preparation

Three copies of the manuscript should be submitted, in double-spaced typing on pages of uniform size with a wide margin on the left.

Some flexibility of presentation will be allowed but authors are urged to arrange the subject matter clearly under such headings as Introduction, Experimental details, Results, Discussion etc. Each paper should have an abstract of 100–200 words.

References should be numbered consecutively (numerals in square brackets) throughout the text and collected together in a reference list at the end of the paper. Journal titles should be abbreviated according to the Chemical Abstracts Service Source Index, 1970 edition, and supplements. The abbreviated title should be followed by volume number, year (in parentheses) and page number.

## Submission of electronic text

The final text should be submitted on a 3.5 in or 5.25 in diskette (in addition to a hard copy with original figures). Double density (DD) or high density (HD) diskettes formatted for MS-DOS or Apple Macintosh compatibility are acceptable, but must be formatted to their capacity before the files are copied on to them. The files should be saved in the native format of the wordprocessing program used. Most popular wordprocessor file formats are acceptable. It is essential that the name and version of the wordprocessing program, type of computer on which the text was prepared, and format of the text files are clearly indicated.

## Illustrations

Line drawings and cyclic or aromatic formulae should be in a form suitable for reproduction. They may be drawn in black ink on drawing paper (letter height, 3–5 mm), but the use of good quality computer-generated figures is encouraged. They should preferably all require the same degree of reduction, and should be submitted on paper of the same size as, or smaller than, the main text to prevent damage in transit. Photographs should be submitted as clear black-and-white prints on glossy paper. Each illustration must be clearly numbered.

Illustrations can be printed in colour when they are judged by the Editor to be essential to the presentation. The publisher and the author will each bear part of the extra costs involved. Further information concerning colour illustrations and the costs to the author can be obtained from the publisher.

Legends to the illustrations must be submitted in a separate list.

All tables and illustrations should be numbered consecutively and separately throughout the paper.

## Proofs

Authors will receive proofs, which they are requested to correct and return as soon as possible. No new material may be inserted in the text at the time of proofreading. All joint communications must indicate the name and full postal address of the author to whom proofs should be sent.

## Further information

All questions arising after the acceptance of manuscripts, especially those relating to proofs, should be directed to: Elsevier Science Ireland Ltd. Elsevier House, Brookvale Plaza, East Park, Shannon, Co. Clare, Ireland. Tel.: +353 61 709600; fax: +353 61 709100.

The full and complete instructions to authors can be found on the World Wide Web: please visit our website which is accessible via the Elsevier Surfaces and Interfaces HomePage at http://www.elsevier.nl/locate/surfaces

## Offprints

Twenty-five offprints will be supplied free of charge to the author(s). Additional offprints can be ordered at prices shown on the offprint order form which accompanies the proofs.

# ภาคผนวก ก8

## Hardness, Tribological Behaviour and Corrosion Performance at the Very Near Surface of Nitrogen Ion-Implanted X5CrNi18.10 Steel

*S. Intarasiri[1], L. D. Yu[1], T. Chudoba[2], H. Reuther[2], U. Rammelt[3] and E. Richter[2]*

[1]Institute for Science and Technology Research and Development,
Chiang Mai University, Chiang Mai 50200, Thailand.
[2]Institute of Ion Beam Physics and Materials Research, D-01314 Dresden, Germany.
[3]University of Technology Dresden, Institute for Physics Chemistry and
Electrochemical, Mommsen Street 13, D-01062 Dresden, Germany.

Published in:

Surface & Coatings Technology 99 (1998) 305-310.

Reprinted from

SURFACE & COATINGS TECHNOLOGY

Surface and Coatings Technology 99 (1998) 305-310

# Hardness, tribological behaviour and corrosion performance at the very near surface of nitrogen ion-implanted X5CrNi18.10 steel

S. Intarasiri [a,*], L.D. Yu [a], T. Chudoba [b], H. Reuther [b], U. Rammelt [c], E. Richter [b]

[a] *Institute for Science and Technology Research and Development, Chiang Mai University, Chiang Mai 50200, Thailand*
[b] *Institute of Ion Beam Physics and Materials Research, D-01314 Dresden, Germany*
[c] *University of Technology Dresden, Institute for Physical Chemistry and Electrochemistry, Mommsen Street 13, D-01062 Dresden, Germany*

Received 7 April 1997; accepted 21 October 1997

ELSEVIER

# SURFACE AND COATINGS TECHNOLOGY



## Scope
The increasing requirement for high technology materials with specific performance characteristics in various types of environments has dictated that these materials possess near-surface properties different from their bulk properties. This journal is a principal forum for the interchange of information on the science, technology and applications of thin and thick coatings and modified surfaces which alter the properties of materials. The scope includes all types of coatings and surface modification techniques (including physical vapour deposition, chemical vapour deposition, electroplating and surface modification by directed energy techniques). Of particular emphasis are the emerging advanced processes such as thermal spraying, sputter deposition, activated reactive evaporation, ion plating, molecular beam epitaxy, ion implantation and pulsed laser surface deposition. Contributions range from original scientific articles concerned with applied research or direct applications of coatings to reviews of current technology in specific areas. Papers are solicited on topics which include one or more of the following areas: (1) characterization of coatings and modified surfaces, which includes the determination of composition, structure, adhesion, and internal stresses; (2) the application of coatings and modified surfaces to alter the mechanical, chemical or optical properties of materials. Mechanical properties include friction, wear, erosion, hardness and load bearing capacity. Chemical properties include corrosion and oxidation. Optical and electro-optical properties include reflectivity, selective absorption and electroluminescence. Particular emphasis is also placed on the emerging surface engineering technologies and coatings with a diversity of applications such as diamond, diamond-like carbon, and cubic boron nitride. Other interdisciplinary areas include thermal barrier coatings and coatings for biomedical applications and materials conservation.

## Abstracting/Indexing Services
This journal is cited by the following services: Engineering Index, FIZ Karlsruhe, Metal Finishing Abstracts, Current Contents — Engineering, Technology and Applied Sciences, Physikalische Berichte, Cambridge Scientific Abstracts, Chemical Abstracts, Fluid Abstracts, Metals Abstracts, Physics Abstracts, PASCAL/Centre National de Recherche Scientifique, Solid State Abstracts.

Pre-publication abstracts of articles in *Surface and Coatings Technology* and other related journals are now available weekly in electronic form via CoDAS, a new direct alerting service in condensed matter and materials science run jointly by Elsevier Science and Institute of Physics Publishing. For details on a free one-month subscription contact Paul Bancroft on fax +44 1179 294318 or e-mail bancroft@ioppublishing.co.uk.

## Publication Information
*Surface and Coatings Technology* (ISSN 0257-8972). For 1998 volumes 96–108 are scheduled for publication. Subscription prices are available upon request from the Publisher. Subscriptions are accepted on a prepaid basis only and are entered on a calendar year basis. Issues are sent by surface mail except to the following countries where Air delivery via SAL mail is ensured: Argentina, Australia, Brazil, Canada, Hong Kong, India, Israel, Japan, Malaysia, Mexico, New Zealand, Pakistan, PR China, Singapore, South Africa, South Korea, Taiwan, Thailand, USA. For all other countries airmail rates are available upon request. Claims for missing issues should be made within six months of our publication (mailing) date.

## Orders, Claims and Product Enquiries
Please contact the Customer Support Department at the Regional Sales Office nearest you:

**New York**
Elsevier Science, P.O. Box 945, New York, NY 10159-0945, USA
Tel.: (+1) 212-633-3730
[Toll free number for North American customers: 1-888-4ES-INFO (437-4636)]
Fax: (+1) 212-633-3680
E-mail: usinfo-f@elsevier.com

**Amsterdam**
Elsevier Science, P.O. Box 211, 1000 AE Amsterdam, The Netherlands
Tel.: (+31) 20-4853757
Fax: (+31) 20-4853432
E-mail: nlinfo-f@elsevier.nl

**Tokyo**
Elsevier Science, 9-15 Higashi-Azabu 1-chome, Minato-ku, Tokyo 106, Japan
Tel.: (+81) 3-5561-5033
Fax: (+81) 3-5561-5047
E-mail: info@elsevier.co.jp

**Singapore**
Elsevier Science, No. 1 Temasek Avenue, #17-01 Millenia Tower, Singapore 039192
Tel.: (+65) 434-3727
Fax: (+65) 337-2230
E-mail: asiainfo@elsevier.com.sg


**US mailing notice**—*Surface and Coatings Technology* (ISSN 0257-8972) is published monthly by Elsevier Science S.A. (PO Box 564, 1001 Lausanne). Annual subscription price in the USA is US$ 4544.00 (valid in North, Central and South America), including air speed delivery. Second class postage rate is paid at Jamaica, NY 11431.
**USA POSTMASTER**: Send address changes to *Surface and Coatings Technology* Publications Expediting, Inc., 200 Meacham Avenue, Elmont, NY 11003.
**AIRFREIGHT AND MAILING** in the USA by Publications Expediting.


## Advertising information
Advertising orders and enquiries may be sent to:
**International**: Elsevier Science, Advertising Department, The Boulevard, Langford Lane, Kidlington, Oxford OX5 1GB, UK. Tel.: +44 (1865) 843 565. Fax: +44 (1865) 843952. **USA and Canada**: Elsevier Science Inc., Mr. Tino DeCarlo, Advertising Sales Director, 655 Avenue of the Americas, New York, NY 10010-5107, USA; Tel.: +1 212 633 3815; Fax: +1 212 633 3820. **Japan**: Elsevier Science Japan, Advertising Department, 1-9-15 Higashi Azabu, Minato-ku, Tokyo 106, Japan. Tel.: +81 3 5561 5033. Fax: +81 3 5561 5047.

ELSEVIER

Surface and Coatings Technology 99 (1998) 305-310

SURFACE & COATINGS TECHNOLOGY

# Hardness, tribological behaviour and corrosion performance at the very near surface of nitrogen ion-implanted X5CrNi18.10 steel

S. Intarasiri [a,*], L.D. Yu [a], T. Chudoba [b], H. Reuther [b], U. Rammelt [c], E. Richter [b]

[a] *Institute for Science and Technology Research and Development, Chiang Mai University, Chiang Mai 50200, Thailand*
[b] *Institute of Ion Beam Physics and Materials Research, D-01314 Dresden, Germany*
[c] *University of Technology Dresden, Institute for Physical Chemistry and Electrochemistry, Mommsen Street 13, D-01062 Dresden, Germany*

Received 7 April 1997; accepted 21 October 1997

**Abstract**

The influence of nitrogen ion implantation on the hardness, tribological behaviour and corrosion performance at the very near surface of polished X5CrNi18.10 steel was studied. The specimens were implanted with 120 keV $N^+$ ions to four different fluences ranging from $10^{16}$ to $10^{18}$ ions $cm^{-2}$. It was found that hardness, tribological behaviour in terms of wear and friction, and corrosion resistance of the specimens strongly depend on the implantation conditions. The greatest improvement in the surface properties of the steel was achieved at doses between $1 \times 10^{17}$ and $5 \times 10^{17}$ ions $cm^{-2}$. Although hardness, wear resistance and friction behaviour were improved noticeably by the implantation, N ion implantation tended to reduce the corrosion resistance of the specimens in $KNO_3$. © 1998 Published by Elsevier Science S.A.

*Keywords:* Nitrogen ion implantation; X5CrNi18.10 steel; Hardness; Tribological behaviour; Corrosion performance

## 1. Introduction

Stainless steels have been widely used in situations where corrosion resistance is required; however, their hardness, wear and friction properties are not particularly good. Ion implantation is an attractive technique for the improvement of metal surfaces, particularly in the small areas, without altering the bulk properties. Near-surface properties in metal surfaces such as hardness, friction and resistance to wear and corrosion are affected by ion implantation. In addition, the surface composition can be altered, leading to the formation of stable or metastable alloys or compounds which cannot often be formed by conventional methods.

Nitrogen is one of the most promising ion species used in ion implantation to improve the surface mechanical and chemical properties of various steels. With normal energies, e.g. 100 keV, implanted N ions penetrate into steels at a depth of about 100 nm and bring about changes in the relevant properties. However, based on conventional testing techniques, as well as considering practical applications, most of the previous work investigated the hardness and wear behaviour of the N ion-implanted steels in depth ranges far beyond the ion-implanted layers. This was due to employing either relatively high loads or long testing periods (e.g. [1,2]). The results are certainly useful and beneficial, but lack detail on the behaviour in the implanted-ion layer region. To provide data to fill the gap in the previously obtained results, this experiment attempted to study the hardness, tribological behaviour and corrosion performance of a N ion-implanted stainless steel, X5CrNi18.10, in the depth region within the implanted-ion layer, using newly developed testing methods.

## 2. Experimental

The samples were mechanically punched out of a X5CrNi18.10 steel sheet (see Table 1 for composition) into rectangular pieces of dimension $15 \times 10 \times 3$ $mm^3$. Before the implantation, the samples were electrochemically polished to a roughness value (Ra) below 30 nm.

A Danfysik ion implanter version 101 was used for the ion implantation. The samples were implanted with

* Corresponding author. Tel: +66 53 943379; Fax: +66 53 222776; E-mail: saweat@istrd.cmu.ac.th.


*PII* S0257-8972(97)00684-1

Table 1
Chemical compositions of X5CrNi18.10 steel [3]

| Fe | C | Si | Mn | P | S | Cr | Ni |
|---|---|---|---|---|---|---|---|
| Balance | <0.07 | 1.00 | 2.00 | 0.045 | 0.030 | 18 | 10 |

Values are shown as percentages.

$N^+$ ions at 120 keV to doses of $5\times10^{16}$, $1\times10^{17}$, $5\times10^{17}$ and $1\times10^{18}$ ions $cm^{-2}$ in a vacuum of $6\times10^{-4}$ Pa. The target temperature measured by a Ni–Cr–Ni thermocouple during the implantation was kept at 150 °C. The ion beam was electrostatically scanned over the entire surface of the samples with a beam current density of about 180–200 μA $cm^{-2}$.

After implantation, the surface of the samples was observed by a scanning electron microscope. The nitrogen depth distribution was determined using Auger electron spectroscopy (AES) combined with argon sputtering. The $Ar^+$ ion beam energy was kept constant at 3 kV with sputtering time-steps of 30 s on a scanned area of 2 $mm^2$. The elements monitored during the profiling were Fe, Ni, Cr and O. The data for N are in the form of relative atomic concentrations estimated from the Auger peak areas.

The hardness measurements of the unimplanted and implanted samples were carried out using an ultramicrohardness tester DUH-202 (Shimadzu) and a Vickers indenter with a tip angle of 136°. The load depth functions obtained by the tester were analysed by the HAERTE program developed by Chudoba [4], which separates plastic and elastic deformation and includes a tip shape correction of the indenter. The program allows the calculation of a depth-dependent ratio of hardness between the implanted and unimplanted sample. In this way the influence of the ions on the hardness can be observed down to a depth of 20 nm. At the maximum load of 10 mN a penetration depth of about 0.3 μm was reached. The loading speed was 0.095 mN $s^{-1}$. At the peak load the load was held constantly for 10 s.

The friction coefficient measurements against a vibrating diamand stylus were performed by a SST-101 scanning scratch tester (Shimadzu). For the measurements a diamond stylus with a tip radius of 10 μm, an amplitude of 100 μm, a down speed of 1 μm $s^{-1}$ and a scratch speed of 2 μm $s^{-1}$ (stage movement perpendicular to the vibration) were used. The maximum load was 100 mN.

The wear performance of the samples was evaluated using an alcohol-lubricated sliding wear tester. The tests were carried out using polished ball-bearings of 3 mm diameter made of 1.3505 (100Cr6) steel which was hardened to 64 HRC (800 HV). The sliding speed was 17 mm $s^{-1}$ and the normal load 1000 mN.

The corrosion of the samples was investigated using electrochemical impedance spectroscopy (EIS). Impedance data were obtained at the open circuit potential with an IM5d impedance measurement system (Zahner-Meßtechnik). The experiments were performed in 0.5 M $KNO_3$ (pH 6–7) with an area of 0.2 $cm^2$ exposed to the solution. The frequency range analysed was 50 kHz to 0.1 Hz and the amplitude of the superimposed a.c. signal was 10 mV.

## 3. Results

Fig. 1 shows scanning electron micrographs of the surfaces of the unimplanted and implanted samples. There were no evident surface changes at doses of $5\times10^{16}$ ions $cm^{-2}$ (Fig. 1a), $1\times10^{17}$ ions $cm^{-2}$ (Fig. 1b) or $5\times10^{17}$ ions $cm^{-2}$ (Fig. 1c), but at the dose of $1\times10^{18}$ ions $cm^{-2}$ (Fig. 1d) large blisters associated with the formation of nitrogen bubbles were observed.

Fig. 2 shows the atomic concentration of nitrogen in the implanted layer of polished X5CrNi18.10 steel, measured by AES, combined with Ar ion sputter etching. At the dose of $5\times10^{16}$ ions $cm^{-2}$ the nitrogen peak concentration in the implanted sample was about 2 at.% at 100 nm depth (Fig. 2a). The peak concentration increased to 4 at.% at a depth of 115 nm (Fig. 2b) and a dose of $1\times10^{17}$ ions $cm^{-2}$. Fig. 2c shows that at a dose of $5\times10^{17}$ ions $cm^{-2}$ the nitrogen peak concentration was 14 at.% at a depth of 80 nm. At the dose of $1\times10^{18}$ ions $cm^{-2}$ two peaks appeared at a depth of 70 nm and 110 nm, respectively, with peak concentrations of 17 and 14 at.% (Fig. 2d).

The effect of the nitrogen ion implantation on the surface hardness of the samples is shown in Fig. 3, in which the depth-dependent ratio of hardness between the implanted samples and the unimplanted sample is given. Nitrogen ion implantation increased the near-surface hardness of the sample up to a depth of about 100 nm by 90% at the dose of $5\times10^{17}$ ions $cm^{-2}$, 30% at $1\times10^{17}$ ions $cm^{-2}$, 20% at $1\times10^{18}$ ions $cm^{-2}$ and 10% at $5\times10^{16}$ ions $cm^{-2}$.

The effect of nitrogen ion implantation on the friction coefficient against a vibrating diamand tip is shown in Fig. 4. The higher the load the deeper the tip penetrated into the sample surface, but up to the maximum load of 100 mN the tip stayed in the implanted layer. The nitrogen ion implantation was able to halve the friction coefficient at the doses of $1\times10^{17}$ ions $cm^{-2}$ and $5\times10^{17}$ ions $cm^{-2}$, in comparison with the unimplanted sample. There was no evidence of a difference in the friction coefficient of the sample implanted with $5\times10^{16}$ ions $cm^{-2}$ and $1\times10^{18}$ ions $cm^{-2}$ compared with the unimplanted sample.

The effect of nitrogen ion implantation on the wear behaviour in the implanted-ion-layer region (Fig. 5 demonstrates the wear-tested depth) is shown in Fig. 6, which displays the volume loss as a function of the

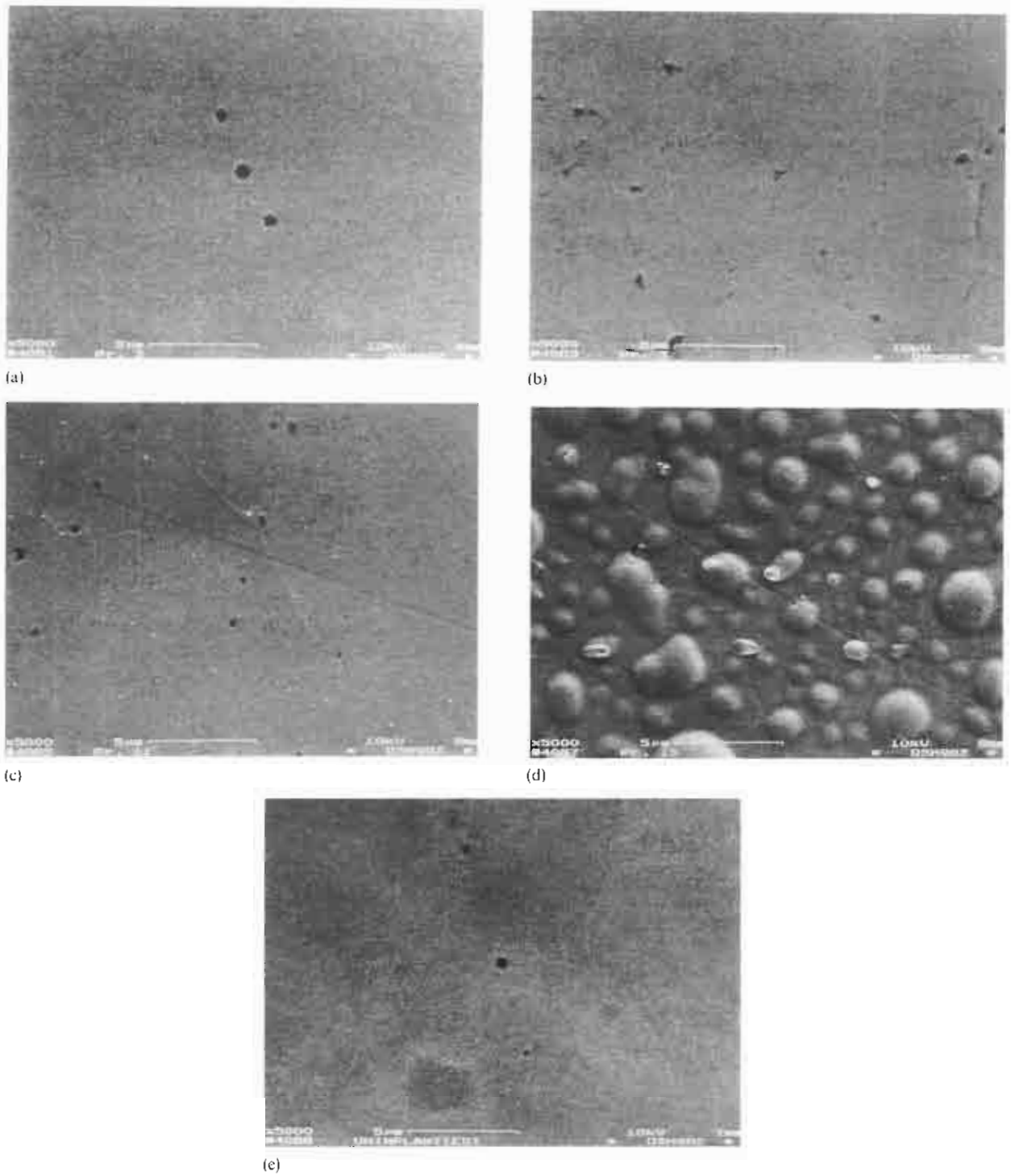


Fig. 1. Scanning electron micrographs of the surface of $N^+$-implanted X5CrNi18.10 steel at a dose of (a) $5 \times 10^{16}$ ions cm$^{-2}$; (b) $1 \times 10^{17}$ ions cm$^{-2}$; (c) $5 \times 10^{17}$ ions cm$^{-2}$; and (d) $1 \times 10^{18}$ ions cm$^{-2}$. For comparison, the scanning electron micrograph of the surface of unimplanted X5CrNi18.10 steel is shown in (e).

sliding distance. At the doses of $5 \times 10^{16}$ ions cm$^{-2}$, $1 \times 10^{17}$ ions cm$^{-2}$ and $5 \times 10^{17}$ ions cm$^{-2}$, the nitrogen ion implantation reduced the volume loss of the implanted surface, but at the dose of $1 \times 10^{18}$ ions cm$^{-2}$ at the starting distance, there was an increase in the volume loss for the implanted surface in comparison with the unimplanted surface, caused by large blisters associated with the formation of nitrogen bubbles.

The effect of the nitrogen ion implantation on the

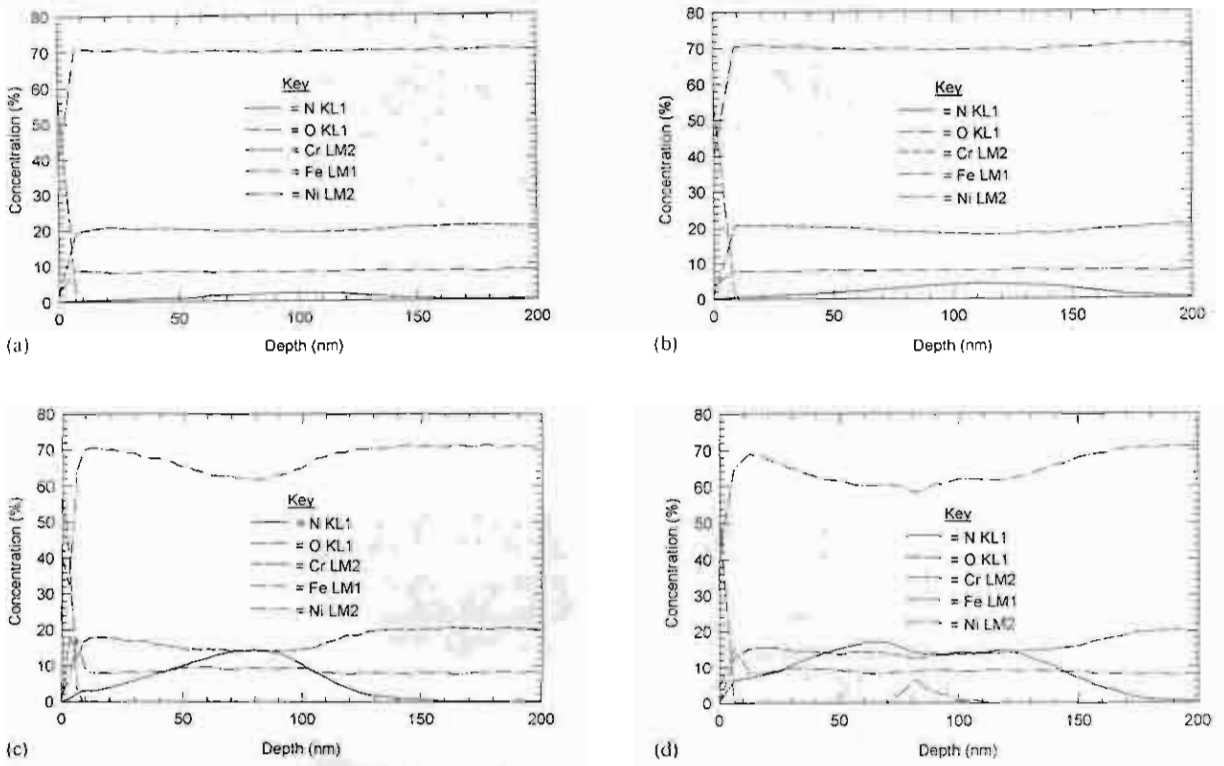


Fig. 2. Depth profiles of nitrogen, oxygen, chromium, iron and nickel in $N^+$-implanted X5CrNi18.10 steel at a dose of (a) $5 \times 10^{16}$ ions $cm^{-2}$; (b) $1 \times 10^{17}$ ions $cm^{-2}$; (c) $5 \times 10^{17}$ ions $cm^{-2}$; and (d) $1 \times 10^{18}$ ions $cm^{-2}$.

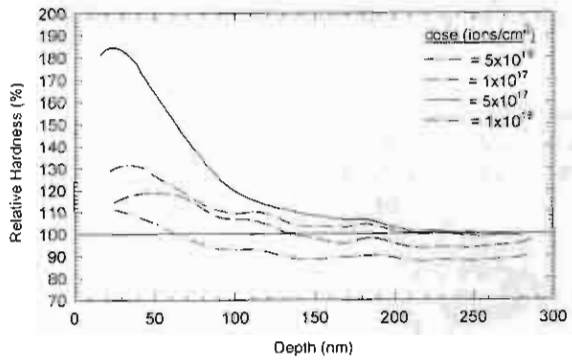


Fig. 3. Depth-dependent ratio of hardness between $N^+$-implanted and unimplanted X5CrNi18.10 steel for different doses.

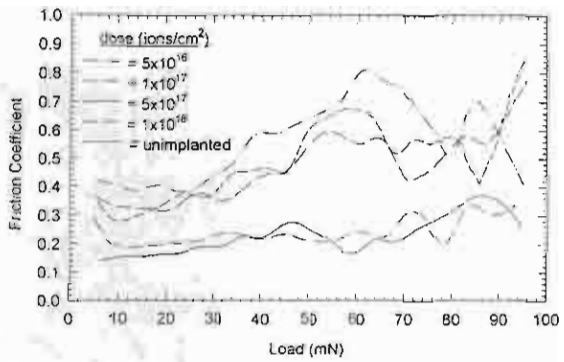


Fig. 4. Load-dependent friction coefficient against a vibrating diamond tip for $N^+$-implanted X5CrNi18.10 steel for different doses.

corrosion behaviour of the sample surfaces is shown in Table 2, which compares the electrical properties of the unimplanted and implanted samples. The corrosion parameters were obtained from the impedance spectra plotted as Bode diagrams [5] in Fig. 7. The impedance spectra can be described by an equivalent circuit for solid metal electrodes, where $R_{pot}$ is the corrosion resistance, $C_{dl}$ the double layer capacity and $K_{diff}$ the diffusion resistance [5]. $R_{pot}$ is inversely proportional to the corrosion rate, i.e. the lower the value of $R_{pot}$ the higher the corrosion rate. As predicted by the corrosion potential ($U_{corr}$), the nitrogen-implanted samples had lower corrosion resistance than the unimplanted sample. With

Table 2
Electrical properties of the surface of the samples

| Dose (ions $cm^{-2}$) | $U_{corr}$ (mV) | $R_{pot}$ (kW) | $C_{dl}$ (μF) | $K_{diff}$ (kW) |
|---|---|---|---|---|
| Unimplanted | −35 | 887 | 3.56 | — |
| $5 \times 10^{16}$ | −192 | 598 | 3.85 | — |
| $1 \times 10^{17}$ | −232 | 470 | 3.03 | — |
| $5 \times 10^{17}$ | −186 | 64 | 1.64 | 520 |
| $1 \times 10^{18}$ | −132 | 73 | 1.15 | 332 |

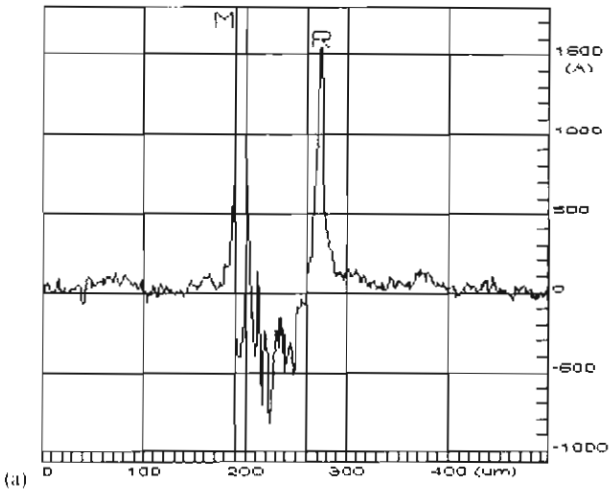


Fig. 5. (a) An example of the profile of a wear trace on the tested sample implanted with a dose of $1 \times 10^{17}$ N ions cm$^{-2}$. The average depth of the trace is less than 60 nm, which is within the implanted N ion layer. For comparison, the wear-trace profile on the unimplanted sample is shown in (b).

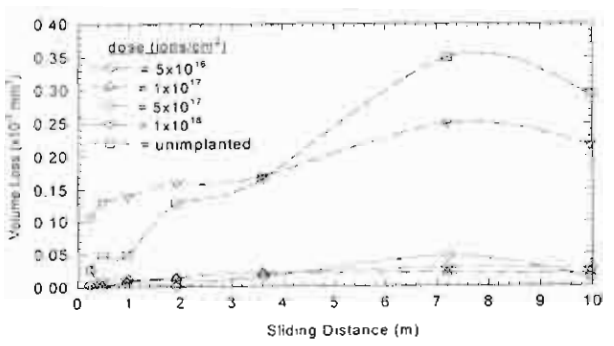


Fig. 6. Dose dependence of volume loss of $N^+$-implanted X5CrNi18.10 steel.

doses of $5 \times 10^{17}$ and $1 \times 10^{18}$ ions cm$^{-2}$ the corrosion rate was very high and diffusion processes occurred additionally in the impedance spectra, indicating that

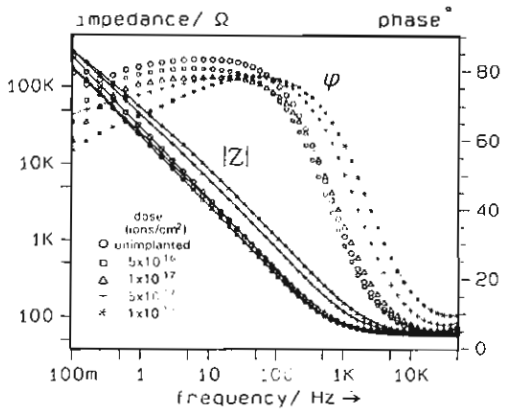


Fig. 7. Bode diagram of $N^+$-implanted X5CrNi18.10 steel.

corrosion products must be transported from the sample surface. The drastic decrease in $R_{pol}$ correlated with the increasing roughness of the surface in the cases of $5 \times 10^{17}$ and $1 \times 10^{18}$ ions cm$^{-2}$.

## 4. Discussion

From the experimental results, it can be seen that N ion implantation is certainly beneficial for the improvement of mechanical properties of X5CrNi18.10 steel, even from the very near surface where the implanted N ions remain. The dose dependence of the hardness, wear and friction of the steel indicates that the greatest improvement in the surface properties of the steel could be obtained at doses between $1 \times 10^{17}$ and $5 \times 10^{17}$ ions cm$^{-2}$ for normal nitrogen ion implantation. Although there were no differences in the influence on friction and wear properties between the two doses, the dose of $5 \times 10^{17}$ ions cm$^{-2}$ produced a higher hardness than did the dose of $1 \times 10^{17}$ ions cm$^{-2}$. The surface hardening due to N ion implantation is mainly contributed by the ion-irradiated very-near-surface region, which is slightly shallower than the N ion projectile range, as shown in Fig. 3. It could be supposed that, besides the contribution from the implanted N ions, which form either interstitial decorating dislocations [6] or hard nitride (e.g. [7]), to strengthen the steel, implantation-induced surface oxide (the oxygen distributed in the very-near-surface region is shown in Fig. 2) may also strongly participate in the hardening, as well as decreasing the friction coefficient by weakening the adhesion between two relatively sliding surfaces [8], as demonstrated in Fig. 4. However, as seen in the figures, this effect is not linearly proportional to the ion dose. For the case of the high-dose N ion-implanted sample, it is believed that because of heavy irradiation damage and nitrogen precipitate bubbles on the top surface, mechanical properties including hardness and tribology were not improved as much as for the medium-dose N

ion-implanted samples. From the comparison shown in Fig. 6, wear of the unimplanted surface initially behaved by breaking through step-by-step, while that of the implanted surface showed a stable evolution. These phenomena indicate and also demonstrate that N ion implantation hardens the steel, beginning from the top surface.

However, the corrosion resistivity decreases with the increasing dose of nitrogen ion implantation, especially if the surface becomes rougher. The fact that the corrosion rate at the very-near-surface region of the steel is increased by the N ion implantation apparently disagrees with some previous published results, which showed a positive effect of N ion implantation on reducing the corrosion speed of iron [9]. However, a universal conclusion cannot simply be drawn without noting the detailed experimental conditions. A chemically inert surface layer formed on the substrate is generally responsible for corrosion protection. In cases where N ion implantation can improve corrosion resistance, this is attributed to the formation of metal nitride (e.g. [10]), but ion implantation also causes irradiation damage on the near-surface regions of the substrate, enhancing the corrosion rate (e.g. [11]). Therefore, the compromise between the formation of the corrosion-resistant compound and the production of ion-beam irradiation damage determines the ion implantation effect on modification of the corrosion property. The present implantaton was performed using the higher beam current density, about one order of magnitude higher than the conventional values, and basically at room temperature. Consequently, heavier irradiation damage and less nitride are supposedly induced [12]. A synthesized result from these factors is then a reduction in corrosion protection. Furthermore, because the testing acid is $KNO_3$, the implanted nitrogen is seemingly inert to the acid as, for example, implanted argon in stainless steel behaving in normal acid solution [13], so that it cannot have much effect on the activity of the acid.

## 5. Conclusions

The hardness, tribological behaviour and corrosion performance of N ion-implanted X5CrNi18.10 steel were studied at the depths of the implanted ion layers using specially designed methods for testing the very-near-surface region. The dose dependence of the property modification was investigated. The noticeable improvement in hardness and tribology, beginning from the top surface, benefited most from the medium-dose ($1.5 \times 10^{17}$ N ions $cm^{-2}$) N ion implantation. The effect of N ion implantation on the corrosion protection of the steel in the acid $KNO_3$ was found to be negative, proportional to the dose, and supposedly attributed to surface irradiation damage and less nitride formation.

## Acknowledgements

S. Intarasiri wishes to thank the staff of the Institute of Ion Beam Physics and Materials Research, Dresden, for their kind support and hospitality, and the Thai Research Fund for the partial support; L.D. Yu wishes to thank the National Science and Technology Development Agency, Thailand, for its support. We are grateful to Dr. T. Vilaithong of the Department of Physics, Chiang Mai University, for his considerate management and beneficial academic help.

## References

[1] G. Dearnaley, in: C.M. Preece, J.K. Hirvonen (Eds.), Practical Applications of Ion Implantation, Ion Implantation Metallurgy, Conference Proceedings, The Metallurgical Society of AIME, 1980, p. 2.
[2] R. Wei, P.J. Wilbur, W.S. Sampath, D.L. Williamson, L. Wang, Lubricat. Engng, April (1991) 326.
[3] Stahlschluessel Taschenbuch, Verlag Stahlschluessel Wegst, Marbach, 1992.
[4] T. Chudoba, Modification of mechanical and chemical surface properties of Mg by ion implantation, PhD Thesis, Technical University of Dresden, Dresden, 1996.
[5] F. Mansfeld, M.W. Kendig, S. Tsai, Corrosion 38 (1982) 570.
[6] G. Dearnaley, Nucl. Instr. Meth. B 50 (1990) 358.
[7] D.L. Williamson, O. Ozturk, S. Glick, R. Wei, P.J. Wilbur, Nucl. Instr. Meth. B 59/60 (1991) 737–741.
[8] J.K. Hirvonen, C.R. Clayton, in: J.M. Poate, G. Foti, D.C. Jacobson (Eds.), Surface Modification and Alloying by Laser, Ion and Electron Beams, Plenum Press, New York, 1983, p. 422.
[9] P.L. Borona, M. Bassoli, G. Cerisola, P.L. De Anna, Nucl. Instr. Meth. 182/183 (1981) 1001.
[10] K.C. Walter, R.A. Dodd, J.R. Conrad, Nucl. Instr. Meth. B 106 (1995) 552.
[11] Xue Jianming, Zhao Weijing, Wang Yugang, Yan Sha, in: J.S. Williams, R.G. Elliman, M.C. Ridgway (Eds.), Proceedings of the 9th International Conference on Ion Beam Modification of Materials (IBMM '95), Canberra, Australia, February 1995, Elsevier Science, Amsterdam, 1996, p. 1041.
[12] T. Fujihana, Y. Okabe, M. Iwaki, Nucl. Instr. Meth. B 39 (1989) 548.
[13] V. Ashworth, W.A. Grant, A.R. Mohammed, R.P.M. Procter, in: C.M. Preece, J.K. Hirvonen (Eds.), The Effect of Ion Implantation on the Aqueous Corrosion Behavior of an Austenitic Stainless Steel, Ion Implantation Metallurgy, Conference Proceedings, The Metallugical Society of AIME, 1980, p. 47.

# Instructions for Authors

## Submission of Papers

Manuscripts (original and two clear copies) should be submitted to one of the Editors:
for authors in the Americas
**Dr. B. D. Sartwell**, Surface Chemistry Branch,
Naval Research Laboratory, Code 6170, Washington,
DC 20375, USA;
and for authors elsewhere
**Professor A. Matthews**, Director, The Research Centre in Surface Engineering, The University of Hull, Cottingham Road, North Humberside, HU6 7RX, UK.

Contributions are accepted on the understanding that the authors have obtained the necessary authority for publication. Submission of a manuscript implies that it is not under consideration for publication elsewhere.

## Types of contributions

— original papers
— invited or contributed reviews on specific topics
— brief communications on topics of immediate interest
— notices of meetings, symposia and short courses
— technical notes for "Current Industrial Practices" section

## Languages

Papers will be published in English. Both English and US spelling are permitted, provided that spelling is consistent within an article.

Authors in Japan please note that information about how to have the English of your paper checked, corrected and improved (*before submission*) is available from: Elsevier Science Japan, Editorial Service, 1-9-15 Higashi Azabu, Minato-ku, Tokyo 106, Japan; Tel.: +81 3 5561 5032; Fax: +81 3 5561 5045.

## Manuscript preparation

Three copies of the manuscript should be submitted, in double-spaced typing on pages of uniform size with a wide margin on the left.

Some flexibility of presentation will be allowed but authors are urged to arrange the subject matter clearly under such headings as Introduction, Experimental details, Results, Discussion etc. Each paper should have an abstract of 100–200 words.

References should be numbered consecutively (numerals in square brackets) throughout the text and collected together in a reference list at the end of the paper. Journal titles should be abbreviated according to the Chemical Abstracts Service Source Index, 1970 edition, and supplements. The abbreviated title should be followed by volume number, year (in parentheses) and page number.

## Submission of electronic text

The final text should be submitted on a 3.5 in or 5.25 in diskette (in addition to a hard copy with original figures). Double density (DD) or high density (HD) diskettes formatted for MS-DOS or Apple Macintosh compatibility are acceptable, but must be formatted to their capacity before the files are copied on to them. The files should be saved in the native format of the wordprocessing program used. Most popular wordprocessor file formats are acceptable. It is essential that the name and version of the wordprocessing program, type of computer on which the text was prepared, and format of the text files are clearly indicated.

## Illustrations

Line drawings and cyclic or aromatic formulae should be in a form suitable for reproduction. They may be drawn in black ink on drawing paper (letter height, 3–5 mm), but the use of good quality computer-generated figures is encouraged. They should preferably all require the same degree of reduction, and should be submitted on paper of the same size as, or smaller than, the main text to prevent damage in transit. Photographs should be submitted as clear black-and-white prints on glossy paper. Each illustration must be clearly numbered.

Illustrations can be printed in colour when they are judged by the Editor to be essential to the presentation. The publisher and the author will each bear part of the extra costs involved. Further information concerning colour illustrations and the costs to the author can be obtained from the publisher.

Legends to the illustrations must be submitted in a separate list.

All tables and illustrations should be numbered consecutively and separately throughout the paper.

## Proofs

Authors will receive proofs, which they are requested to correct and return as soon as possible. No new material may be inserted in the text at the time of proofreading. All joint communications must indicate the name and full postal address of the author to whom proofs should be sent.

## Further information

All questions arising after the acceptance of manuscripts, especially those relating to proofs, should be directed to: Elsevier Science Ireland Ltd. Bay 15K, Shannon Industrial Estate, Shannon, Co. Clare, Ireland; Tel.: +353 61 471944; Fax: +353 61 472144.

The full and complete instructions to authors can be found on the World Wide Web: please visit our website which is accessible via the Elsevier Surfaces and Interfaces HomePage at http://www.elsevier.nl/locate/surfaces

## Offprints

Twenty-five offprints will be supplied free of charge to the author(s). Additional offprints can be ordered at prices shown on the offprint order form which accompanies the proofs.


0257-8972/98/$19.00



Printed in The Netherlands
– The paper used in this publication meets the requirements of ANSI/NISO Z39.48-1992 (Permanence of Paper)

# ภาคผนวก ก9

## Surface Modification of Tool Steels by Combined Cr- and N-Ion Implantation

*L. D. Yu[1], T. Vilaithong[2], B. Yotsombat[2], S. Thongtem[2], J. G. Han[3] and J. S. Lee[3]*

[1]Institute for Science and Technology Research and Development,
Chiang Mai University, Chiang Mai 50200, Thailand.
[2]Department of Physics, Faculty of Science,
Chiang Mai University, Chiang Mai 50200, Thailand.
[3]Department of Metallurgical Engineering, Sung Kyun Kwan University,
300 Chunchun-dong, Jangan-ku, Suwan, South Korea.

**Published in:**

Surface & Coatings Technology 103-104 (1998) 328-333.

ELSEVIER

Surface and Coatings Technology 103–104 (1998) 328–333

SURFACE & COATINGS TECHNOLOGY

# Surface modification of tool steels by combined Cr- and N-ion implantation

L.D. Yu [a,*], T. Vilaithong [b], B. Yotsombat [b], S. Thongtem [b], J.G. Han [c], J.S. Lee [c]

[a] *Institute for Science and Technology Research and Development, Chiang Mai University, Chaing Mai 50200, Thailand*
[b] *Department of Physics, Faculty of Science, Chiang Mai University, Chiang Mai 50200, Thailand*
[c] *Department of Metallurgical Engineering, Sung Kyun Kwan University, 300 Chunchun-dong, Jangan-ku, Suwon, South Korea*

**Abstract**

High and low Cr-content tool steels, SKD11 and SKS3, are implanted successively with 50 keV Cr-ions and 90 keV $N_2$-ions to fluences of $4\times10^{17}$ $Cr^+$ $cm^{-2}$ and $4\times^{17}$ $N^+$ $cm^{-2}$. Microhardness and wear tests, in either dry air or diluted $NaCl+H_2SO_4$ solution environments, are used to investigate the effects of the multiply ion-implanted steel surface modification; these results are compared with singly Cr- and N-ion-implanted surfaces. The role of Cr-ion implantation in improving hardness and wear resistance of the steels in a dry-air environment is inferior to that of N-ion implantation, even affecting the co-implantation effectiveness on increasing hardness and wear resistance. However, combined Cr- and N-ion implantation can more positively enhance wear resistance in the salt–acid solution environment for the low-Cr steel than the high-Cr steel. XRD analysis supplies evidence for an explanation of the results. © 1998 Elsevier Science S.A.

*Keywords:* Cr + N-ion co-implantation; Microhardness; Tribology; Diluted salt-acid solution; Tool steels

## 1. Introduction

The effects of adding nitrogen and chromium into steels on the modification of mechanical and chemical properties are well known: N plays a role in improving hardness and tribological behavior and Cr contributes to raising corrosion resistance. N- or Cr-ion implantation of steels for materials modification has been widely and intensively investigated, and results have confirmed the modification effects [1]. It was proposed that by combining Cr- and N-ion implantations in steels one might obtain dual benefits in both mechanical and chemical property improvements, probably due to the formation of Cr–N. Results from previous work (e.g. see Refs. [2,3]) demonstrated some of the merits of the co-implantation, but still some ambiguities remained, particularly the effect on the modification of tribology. The experiment reported in this paper was designed to investigate Cr + N-ion co-implantation and its effect on hardness and wear behavior in dry air or salt–acid solution environments for tool steels in different conditions, such as high and low chromium contents and whether heat-treated or not.

* Corresponding author.


*PII* S0257-8972(98)00409-5

## 2. Experimental

Samples of heat-treated and untreated high-Cr tool steel, SKD11, and low-Cr tool steel, SKS3, were prepared into Ø20 mm × 3 mm disks with a mirror-surface finish. (See Table 1 for chemical compositions and Table 2 for the heat treatment processes.) The sample surfaces were implanted with 50 keV Cr-ions to $4\times10^{17}$ $Cr^+$ $cm^{-2}$ followed by 90 keV $N_2$-ions to $4\times10^{17}$ $N^+$ $cm^{-2}$, as shown in Table 3. Microhardness and tribology tests were then performed on the samples. A digital microhardness tester (MXT-α, Matsuzawa) was used for hardness testing with normal loading of 5 gf and varying loads from 1 to 50 gf for some tests. Average Knoop hardness numbers (kilograms per square millimeter) with deviations were automatically output by the tester software after testing points randomly distributed on the sample surface. A pin-on-disk-type tribometer (ISC-200, Implant Sciences) was applied for wear testing. The testing environment was either dry air or diluted $NaCl$(3 wt%) + $H_2SO_4$ (pH = 3.00) solution. Testing parameters were chosen to be: 5 or 8 cm $s^{-1}$ sliding speed, WC or 52100-steel ball, 500 gf load and a total of $(1–2)\times10^4$ rotations. X-ray diffraction (XRD) was used to analyze for the formation of

Table 1
Chemical compositions and application examples of the tool steels

| Steel: JIS (AISI) | Chemical composition (%) | | | | | | | | Typical applications |
|---|---|---|---|---|---|---|---|---|---|
| | C | Si | Mn | Cr | Mo | W | V | Ni | |
| SKD11 (D2) | 1.5 | 0.3 | 0.4 | 12.0 | 1.0 | | 0.4 | 0.5 | die, roller, shear blade, plastic mold, gage, etc. |
| SKS3 (O1) | 1.0 | 0.3 | 1.0 | 0.8 | | 0.8 | | | die, gage, tap, roll, shear blade, cutter, plastic mold |

Table 2
Heat treatment processes of the steel samples

| Steel | Preheating | | Hardening | | Quenching media | Tempering | |
|---|---|---|---|---|---|---|---|
| | Temp. (°C) | Time (min) | Temp. (°C) | Time (min) | | Temp. (°C) | time (h) |
| SKD11 | 850 | 5 | 1050 | 15 | oil | 150 | 1+1 |
| SKS3 | 650 | 5 | 850 | 15 | oil | 150 | 1+1 |

Table 3
Ion implantation data of the steel samples, microhardness and pin-on-disk wear testing results

| Steel (JIS) | Heat treatment | Ion implantation species (energy) | HK (kg mm$^{-2}$) | Wear rate ($10^{-6}$ mm$^3$) |
|---|---|---|---|---|
| SKD11 | treated | — | 520 | 0.25, 0.20(ac1) |
| | | $N_2$ (90 keV) | 818 | 0.10/0.24(ac1) |
| | | Cr (50 keV) | 709 | |
| | | Cr (50 keV) + $N_2$ (90 keV) | 860 | 0.20, 0.17(ac1), 0.45(ac2) |
| | untreated | — | 250 | 8.50 |
| | | $N_2$ (90 keV) | 371 | 0.20 |
| | | Cr (50 keV) | 280 | |
| | | Cr (50 keV) + $N_2$ (90 keV) | 341 | 0.25 |
| SKS3 | treated | — | 510 | 0.12 |
| | | $N_2$ (90 keV) | 620 | 0.09, 0.50(ac2) |
| | | Cr (50 keV) | 577 | |
| | | Cr (50 keV) + $N_2$ (90 keV) | 595 | 0.14/0.20(ac2) |
| | untreated | — | 260 | 0.23 |
| | | $N_2$ (90 keV) | 295 | 0.17 |
| | | Cr (50 keV) | 270 | |
| | | Cr (50 keV) + $N_2$ (90 keV) | 286 | 0.10 |

The Knoop hardness number (HK) data were obtained under a testing load of 5 gf. The wear rate data without any notes were under testing conditions of dry-air environments, WC ball, 5 cm s$^{-1}$ sliding speed, 500 gf load and total $10^4$ cycles; those with (ac1) were under the diluted salt acid solution, 52100-steel ball, 4 cm s$^{-1}$ sliding speed, 500 gf load and total $2 \times 10^4$ cycles; those with (ac2) were under the diluted salt acid solution, 52100-steel ball, 8 cm s$^{-1}$ sliding speed, 500 gf load and total $10^4$ cycles.

compounds or phases and an image microscope was used to observe the sample surfaces.

## 3. Results and discussion

Data for microhardness and wear testing are shown in Table 3, and conclusive results with relevant discussion are described below.

### 3.1. Microhardness

#### 3.1.1. Hardness changes due to different ion-species implantation

Either N-, or Cr-, or Cr + N-ion implantation can increase the hardness, but the single Cr-ion implantation makes less improvement than the single N-ion implantation. Even the effect on hardening from the Cr + N-ion co-implantation is lower than that from the single N-ion

implantation in most cases. This agrees with the result of Ref. [2], indicating that Cr-ion implantation in tool steels does not produce a significant hardening effect compared with N-ion implantation. The reason may depend on the hardening mechanisms. N-ions strengthen the implanted steels by either interstitial hardening [4] or nitride precipitate hardening [5], whereas Cr-ion implantation of steels relies on forming hard Cr-compounds. This can be demonstrated by the fact that Cr-ion-implanted heat-treated steels show a greater hardness increase than untreated steels, as shown in Table 3. This is because the heat-treated steels, which are quenched in oil, contain a high carbon content in the near-surface region, so that the implanted Cr, as a carbide-forming element [6], can form Cr–C to harden the steel surface. This contrasts with the untreated steels which, having less surface carbon, cannot provide the high probabilities for forming Cr–C.

### 3.1.2. Hardness comparison of high- and low-Cr steels

As shown in Fig. 1 and Table 4, it is found that the high-Cr steel, SKD11, gains in surface hardness more from the co-implantation than the low-Cr steel, SKS3. This is probably due to the formation of chromium-nitride in the implanted high-Cr steel contributing to the hardening.

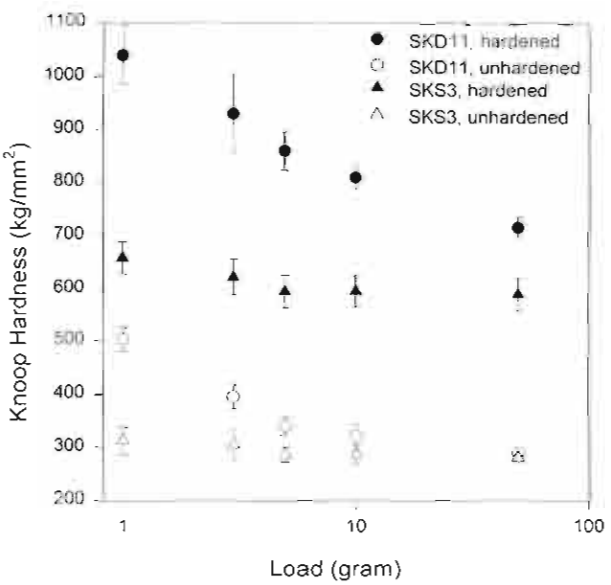


Fig. 1. Knoop hardness of Cr+N-ion co-implanted steels tested with various loads: 1, 3, 5, 10 and 50 g.

### 3.1.3. Hardness comparison of heat-treated and untreated steels

Fig. 1 and Table 4 also show that the hardness of the heat-treated steel samples is increased due to the co-implantation more than that of the untreated steel samples. This is also believed to be related to the formation of large levels of chromium-carbide in the heat-treated steels.

## 3.2. Wear behavior

### 3.2.1. Wear rates under dry-air environment

From Table 3, it is seen that, in most cases, particularly for the heat-treated steels, the effect on improving wear resistance of the steels from the co-implantation is less than that from single N-ion implantation. A careful observation of the data for unhardened steels shows that for high-Cr steel the co-implantation results in a wear rate which is slightly higher than with the single N-ion implantation; however, for the low-Cr steel the co-implantation leads to a wear rate lower than for N-ion implantation. XRD patterns displayed in Fig. 2 show that ε-(Fe,Cr)N forms in non-heat-treated steels but not in heat-treated steels. This may explain why the heat-treated steels produce a negative result. A greater number of precipitates in the wear track on the low-Cr steel samples than on the high-Cr steel sample, as shown in the photomicrographs in Fig. 3, may better protect the low-Cr steel surface from wear.

### 3.2.2. Wear rates under salt–acid solution environment

As seen in Table 3 and Fig. 4, however, co-implantation shows a greater effect on reducing wear under the testing condition of diluted salt–acid solution than the single N-ion implantation, which produces even higher wear rates than no implantation. It is indicated that nitrogen interstitials decorating defects [7] only mechanically

Table 4
Comparisons for hardness between the Cr+N-ion co-implanted high-Cr steel and low-Cr steel

| Steel | Heat treatment | $\Delta HK/HK_0$(5g) (%) | HK(1g)/HK(5g) |
|---|---|---|---|
| SKD11 (high-Cr) | treated | 65 | 1.21 |
| | untreated | 36 | 1.47 |
| SKS3 (low-Cr) | treated | 17 | 1.11 |
| | untreated | 10 | 1.10 |

$\Delta HK = HK - HK_0$, where HK is the hardness of the implanted samples, and $HK_0$ that of unimplanted samples, tested with a load of 5 gf (data from Table 3). HK(1g) is under a load of 1 gf, and HK(5g) under 5 gf (data from Fig. 1).

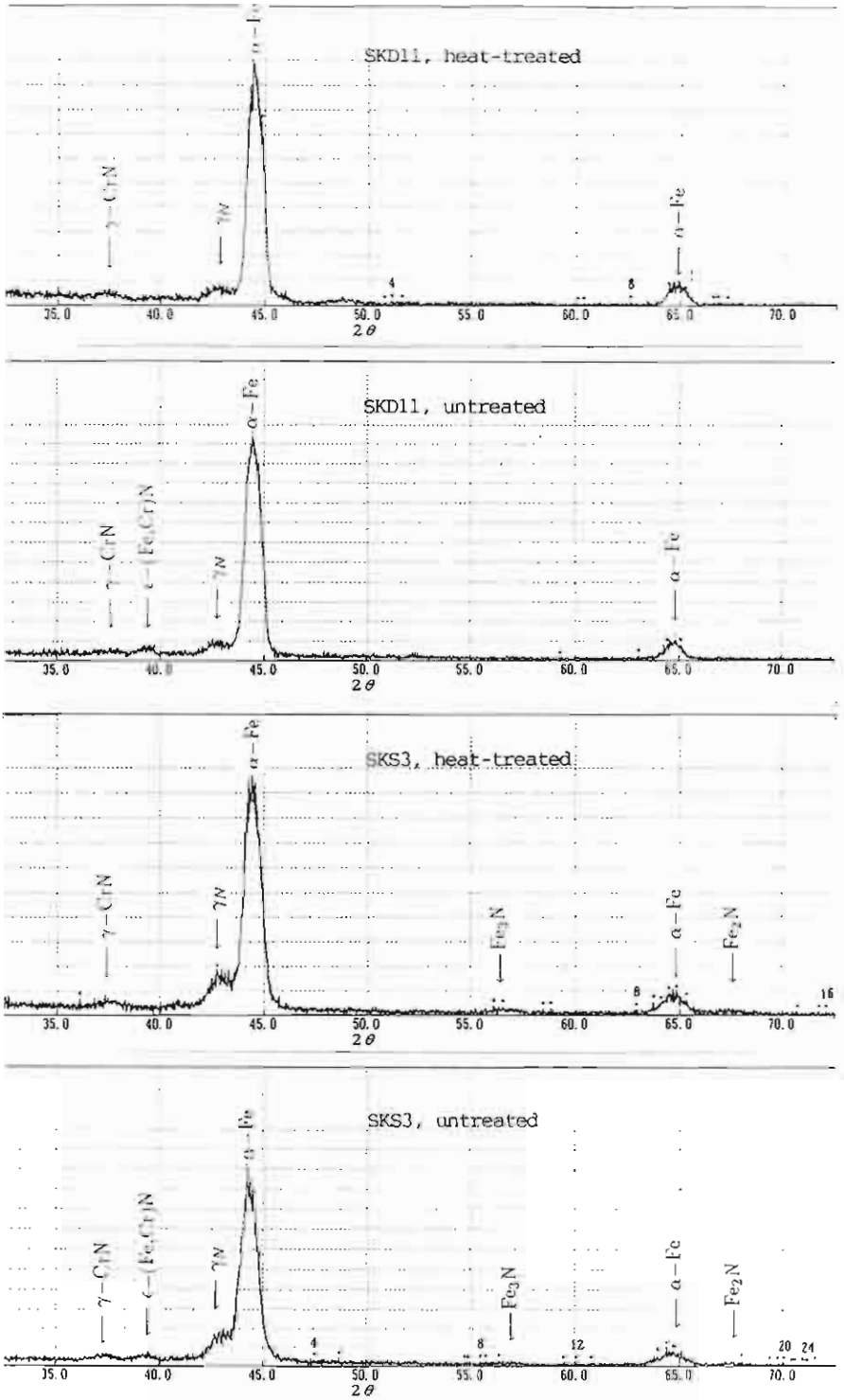


Fig. 2. XRD patterns of Cr + N-ion co-implanted steel samples.

strengthen the substrate, but have limited ability to protect the substrate from chemical affinity attacks.

*3.2.3. Comparison of wear rates of high- and low-Cr steels under salt–acid solution environment*

The low-Cr steel, SKS3, receives more of a benefit from the co-implantation than the high-Cr steel, SKD11, as shown in Table 3 and Fig. 4. For the high-Cr steel, because of the rich Cr content, which will trap N-ions to form Cr–N due to chromium also being a nitride-forming element [6], N-ions cannot penetrate deeper inside the substrate. But for the low-Cr steel, saturation by the trapping of Cr with N-ions forming Cr–N will not impede more N-ions from travelling to deeper

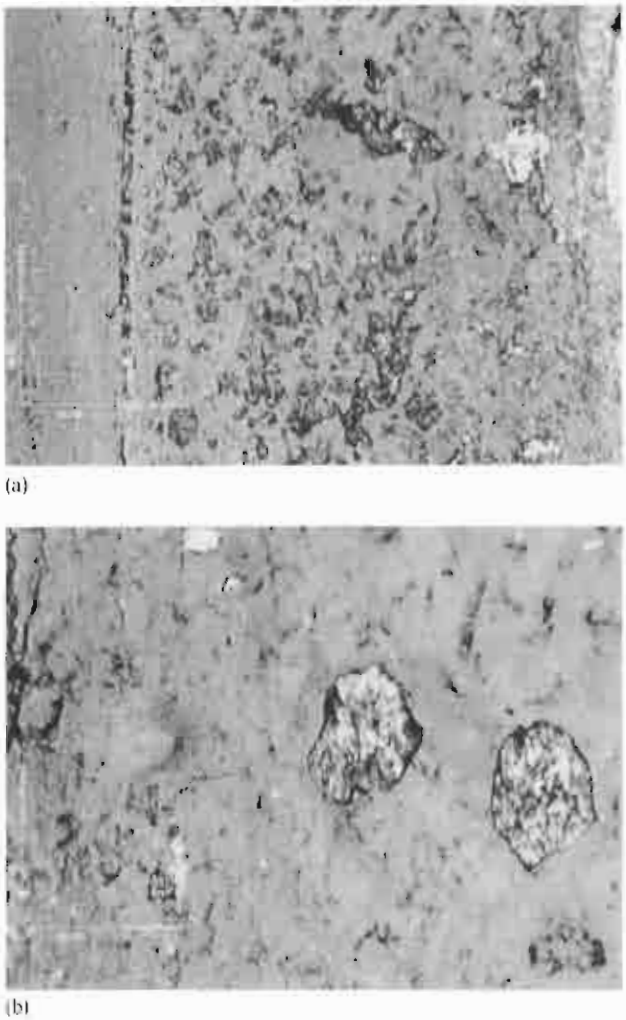

Fig. 3. Photomicrographs of wear tracks on the non-heat-treated steel samples tested in a dry-air environment. A greater number of nitride precipitates are seen on the SKS3 (low Cr) sample (a) than on the SKD11 (high Cr) sample (b).

regions in the substrate subsurface [8]. XRD analysis found Fe–N formed in SKS3 steel but no nitride in SKD11, as shown in Fig. 2. Now that both steels have Cr–N, the one having Fe–N certainly has higher wear resistance.

## 4. Conclusions

The effects of Cr- and N-ion implantation in tool steels on the modification of hardness and wear behavior have been studied. Comparisons have been made between single Cr-ion and N-ion implantation and Cr + N-ion co-implantation, under the wear conditions of either dry air or a diluted salt–acid solution environment, using high- and low-Cr steels in the heat-treated and untreated states. From the study, it is concluded that although implanting Cr-ions in various ways can

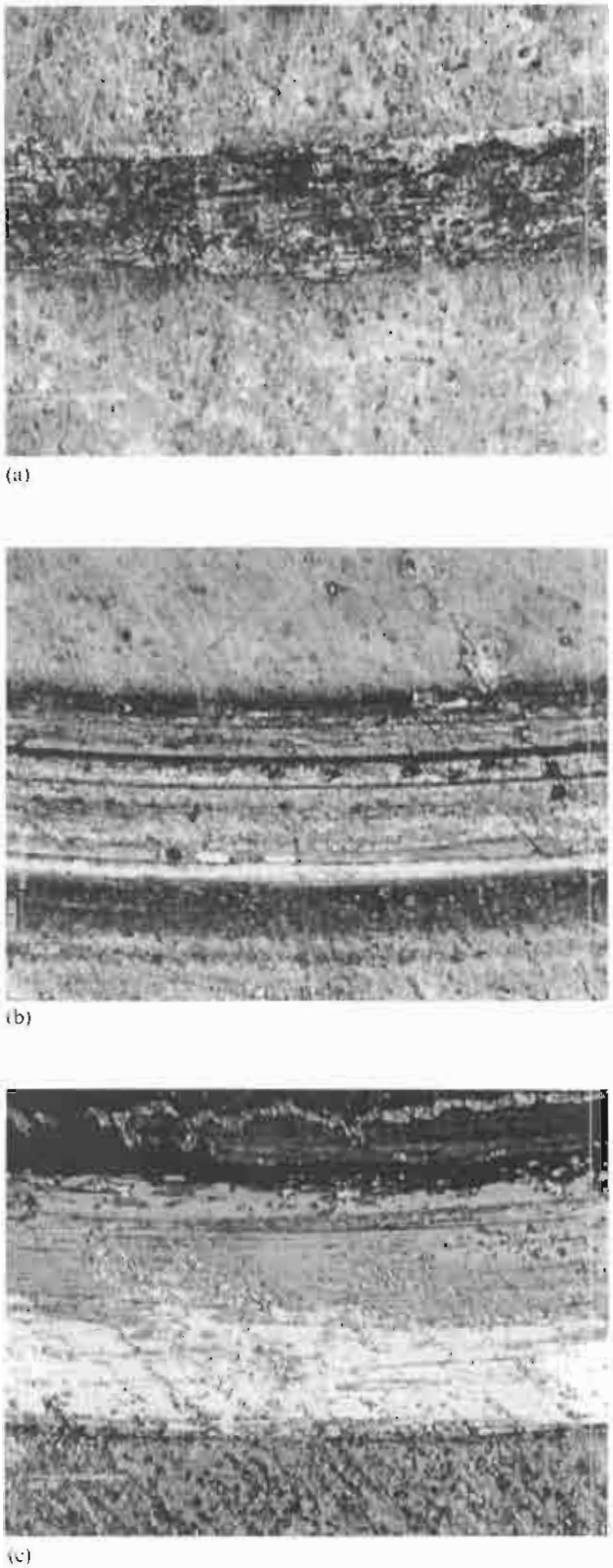

Fig. 4. Photomicrographs of wear tracks on the heat-treated steel samples tested in the salt–acid solution environment. The track on the Cr + N-ion co-implanted SKS3 sample (a) is narrower than that on either the singly N-ion-implanted SKS3 sample (b) or the Cr + N-ion co-implanted SKD11 sample (c).

truly help the steel hardness enhancement, its role in improving mechanical and chemical properties of the steels is still debatable. Detailed conclusions are listed below.

Implanting Cr-ions, whether singly or in combination with N-ions, in tool steels is generally not significantly helpful (and sometimes even deleterious) to hardening and improvement of wear protection in a dry-air environment compared with implanting N-ions alone. However, Cr- and N-ion co-implantation has a positive effect on reducing wear of steels in a diluted salt–acid solution environment compared with single N-ion implantation.

High-Cr steel has a greater hardness improvement from the co-implantation than low-Cr steel, whereas the low-Cr steel receives greater improvement in wear resistance in the diluted salt–acid solution environment than the high-Cr steel.

The wear behavior of the co-implanted steels in a dry-air environment depends on the Cr content and heat treatment. Co-implantation provides the heat-treated steels with less improvement in wear resistance than single N-ion implantation. For untreated steels, low-Cr steel has better wear protection after co-implantation than the high-Cr steel.

## Acknowledgements

We are grateful to Dr. Kim of the Korean Atomic Energy Research Institute for performing the Cr-ion implantation. This work was supported by the National Science of Technology Development Agency, Thailand, the Thai Research Fund and the Thailand–Korea Cooperative Program on Ion Implantation Modification of Precision Tools.

## References

[1] J.K. Hirvonen, C.R. Clayton, in: J.M. Poate, G. Foti, D.C. Jacobson (Eds), Surface Modification and Alloying by Laser, Ion and Electron Beams, Plenum Press, 1983, p. 422.
[2] F. Alonso, J.L. Viviente, J.I. Onate, B. Torp, B.R. Nielsen, Nucl. Instrum. Methods B: 80–81 (1993) 254–257.
[3] M. Kopcewicz, J. Jagielski, A. Turos, G. Gawlik, Nucl. Instrum. Methods B: 80–81 (1993) 327–331.
[4] G. Dearnaley, Nucl. Instrum. Methods B: 50 (1990) 358–367.
[5] D.L. Williamson, O. Ozturk, S. Glick, R. Wei, P.J. Wilbur, Nucl. Instrum. Methods B: 59–60 (1991) 737–741.
[6] K.-E. Thelning, Steel and its Heat Treatment, Butterworths, London, 1978 (reprint).
[7] G. Dearnaley, in: C.M. Preece, J.K. Hirvonen (Eds), Practical Applications of Ion Implantation, Ion Implantation Metallurgy, Conference Proceedings, The Metallurgical Society of AIME, 1980, p. 2.
[8] F.A. Smidt, G.K. Hubler, Nucl. Instrum. Methods B: 80–81 (1993) 207–216.

# ภาคผนวก ก10

## N-Ion Implantation Assisted by Preparative and Closing Implantation For Surface Modification of Tool Steel

*T. Vilaithong[1], L. D. Yu[2], P. Vichaisirimongkol[2], G. Rujijanagul[1] and T. Sonkaew[1]*

[1]Department of Physics, Faculty of Science,
Chiang Mai University, Chiang Mai 50200, Thailand.
[2]Institute for Science and Technology Research and Development,
Chiang Mai University, Chiang Mai 50200, Thailand.

Published in:

Nuclear Instruments and Methods in Physics Research B 148 (1999) 830-835.

Reprinted from

NIM B

Beam Interactions with Materials & Atoms

Nuclear Instruments and Methods in Physics Research B 148 (1999) 830–835

# N-ion implantation assisted by preparative and closing implantation for surface modification of tool steel

T. Vilaithong [a], L.D. Yu [b,*], P. Vichaisirimongkol [b], G. Rujijanagul [a], T. Sonkaew [a]

[a] *Department of Physics, Faculty of Science, Chiang Mai University, Chiang Mai 50200, Thailand*
[b] *Institute for Science and Technology Research and Development, Chiang Mai University, Chiang Mai 50200, Thailand*

ELSEVIER

# BEAM INTERACTIONS WITH MATERIALS AND ATOMS
## Nuclear Instruments and Methods in Physics Research – Section B



**Aims and scope**

Section B of Nuclear Instruments and Methods in Physics Research (NIM B) provides a special forum for the discussion of all aspects of the interaction of energetic beams with atoms, molecules and aggregate forms of matter. This includes ion beam analysis and ion beam modification of materials, as well as studies of the basic interaction mechanisms of importance for this work. The Editors invite submission of both theoretical and experimental papers of original research in this area.




**Abstracted/indexed in:**

Current Contents: Engineering, Technology and Applied Sciences; EI Compendex Plus; Engineering Index; INSPEC; Physics Briefs.



**Subscription information 1999**

Volumes 147–159 of Nuclear Instruments and Methods in Physics Research – Section B (ISSN 0168-583X) are scheduled for publication. A combined subscription to NIM A volumes 420-437 and NIM B volumes 147–159 is available at a reduced rate. Subscriptions are accepted on a prepaid basis only and are entered on a calendar year basis. Issues are sent by SAL (Surface Air Lifted) mail wherever this service is available. Airmail rates are available upon request.

*Orders, claims, and product enquiries:* Please contact the Customer Support Department at the Regional Sales Office nearest to you:

*New York:* Elsevier Science, P.O. Box 945, New York, NY 10159-0945, USA; tel +1 212 633 3730 (Toll free number for North American customers: 1-888-4ES-INFO (437-4636)), fax +1 212 633 3680, e-mail usinfo-f@elsevier.com

*Amsterdam:* Elsevier Science, P.O. Box 211, 1000 AE Amsterdam, The Netherlands; tel +31 20 485 3757, fax +31 20 485 3432, e-mail nlinfo-f@elsevier.nl

*Tokyo:* Elsevier Science K.K., 9-15, Higashi-Azabu 1-chome, Minato-ku, Tokyo 106, Japan; tel +81 3 5561 5033, fax +81 3 5561 5047, e-mail info@elsevier.co.jp

*Singapore:* Elsevier Science, No. 1 Temasek Avenue, #17-01 Millenia Tower, Singapore 039192; tel +65 434 3727, fax +65 337 2230, e-mail asiainfo@elsevier.com.sg

*Rio de Janeiro:* Elsevier Science, Rua Sete de Setembro 111/16 Andar, 20050-002 Centro, Rio de Janeiro – RJ, Brazil; phone: (+55) (21) 509 5340; fax: (+55) (21) 507 1991; e-mail: elsevier@campus.com.br [Note (Latin America): for orders, claims and help desk information, please contact the Regional Sales Office in New York as listed above].



**US Mailing notice:** Nuclear Instruments and Methods in Physics Research – Section B (ISSN 0168-583X) is published monthly (for five months of the year), semi-monthly in February, April, June, July and September, and three times a month in January and May, by Elsevier Science B.V., Molenwerf 1, P.O. Box 211, 1000 AE Amsterdam, The Netherlands. Annual subscription price in the USA is US$ 6409 (valid in North, Central and South America only), including air speed delivery. Periodicals postage paid at Jamaica, NY 11431.

**USA Postmasters:** Send address changes to Nuclear Instruments and Methods in Physics Research – Section B, Publications Expediting, Inc., 200 Meacham Avenue, Elmont, NY 11003. Airfreight and mailing in the USA by Publications Expediting Inc.

Printed in The Netherlands

North-Holland, an imprint of Elsevier Science

ELSEVIER

Nuclear Instruments and Methods in Physics Research B 148 (1999) 830–835

NIM B
Beam Interactions with Materials & Atoms

# N-ion implantation assisted by preparative and closing implantation for surface modification of tool steel

T. Vilaithong [a], L.D. Yu [b,*], P. Vichaisirimongkol [b], G. Rujijanagul [a], T. Sonkaew [a]

[a] *Department of Physics, Faculty of Science, Chiang Mai University, Chiang Mai 50200, Thailand*
[b] *Institute for Science and Technology Research and Development, Chiang Mai University, Chiang Mai 50200, Thailand*

**Abstract**

The study aims at investigating the effect of auxiliary preparative and closing implantations in hardened tool steels on surface tribology modification. Samples of a martensitic tool steel, SKD11, are triply implanted with ions of N or Ar at higher energies, N at the normal energy, and N, BF and $CO_2$ at lower energies. The ion implantations result in dramatic increases of hardness and wear resistance to the samples in comparison with single N-ion implantation and double ion implantation. Analysis of ion depth profiles and surface compositions and microstructures is performed to reveal the mechanisms. It can be concluded that the improvement of the mechanical properties can be attributed to the deepening in the ion penetration and the forming of compound covers at the near surface region. 

*PACS:* 62.20.Qp; 68.55.Ln; 81.05.Bx; 81.40.–z
*Keywords:* Preparative implantation; Closing implantation; Hardened tool steel; Tribology; Microhardness; Wear rate

## 1. Introduction

N-ion implantation has long been investigated for modifying mechanical properties, such as hardness and wear rate, of steels. N-ion implantation of hardened steels has commanded great interest [1] not only because of its practical application but also its different characteristics from implantation of unhardened steels [2]. The implanted N-ion depth profiles indicate that the hardened steels have a lower ability in retaining N-ions than the unhardened steels [3], so that they normally exhibit difficulties in gaining comparable improvement in tribology from N-ion implantation. Preparative surface treatment and implantation have been applied prior to normal N-ion implantation to improve the ability of the hardened steels to retain more nitrogen ions [4]. Auxiliary closing implantation is now added to the implantation procedure in an attempt to form a compound cover at the near surface region to close any paths for the normal implanting ions to escaping (diffusing) out, as well as to construct a hard layer which strengthens the normally implanted area.

* Corresponding author. Tel.: +66 53 943379; fax: +66 53 222776; e-mail: yuld@istrd.cmu.ac.th

0168-583X/98/$ – see front matter 
PII: S0168-583X(98)00882-9

Table 1
The chemical compositions of the SKD11 (D-2) tool steel

| C | Si | Mn | Cr | Mo | V | Ni |
|---|---|---|---|---|---|---|
| 1.5 | 0.3 | 0.4 | 12.0 | 1.0 | 0.4 | 0.5 |

## 2. Experiment

Well-surface-finished (0.3 μm) samples of hardened SKD11 (AISI D-2) steel (the chemical compositions are shown in Table 1 and the heat treatment process is displayed in Table 2) were preparatively implanted with higher-energy N-ions or Ar-ions, then normally implanted with 120 keV $N_2$-ions, and finally implanted with lower-energy BF, or $N_2$, or $CO_2$ ions (the triple ion implantation will sometimes be referred to as preparative-plus-closing ion implantation), as summarized in Table 3. The ion implantations were carried out using the 150 kV, mass-analyzed heavy ion implantation facility at Chiang Mai University [5]. The implantation temperatures at the target did not exceed 100°C.

The implanted samples together with unimplanted ones underwent mechanical property testing. A digital microhardness tester (MXT-α, Matzuzawa) using the Knoop scale tested surface hardness by applying a load varying from 1 to 50 g. A pin-on-disk wear tester (ISC-200 Tribometer, Implant Sciences) using WC balls tested wear behavior under the following conditions, 500 g load, 4.8 cm/s sliding speed, and 10 000 total-rotations. The wear rates were evaluated based on the relevant international standard [6].

The ion depth profiles were analyzed using either Auger electron spectroscopy (AES)(mostly) or secondary ion mass spectrometry (SIMS) (only for the samples implanted with Ar-ions). The surface microstructure was characterized and observed using X-ray diffraction (XRD) (Cu, $K_\gamma$) and Scanning electron microscopy (SEM).

## 3. Results and discussion

Table 3 shows the measured microhardness (under the load of 1 g) and the derived wear rate of the ion-implanted samples compared with the data of the unimplanted sample.

As can be seen from the table, as well as Fig. 1, which shows microhardness tested with varying load, the preparative-plus-closing ion implantation increases the hardness drastically in comparison with the single and double ion implantations. The effect of the preparative implantation depends on the ion species. Nitrogen performs better than argon owing to the fact that the N-ions are able to cause both radiation damage and structural strengthening whereas the Ar-ions create only damage. The effect from the closing implantation seems to be more pronounced than the preparative implantation. Proper selection of the closing implanted ion species, such as boron, carbon or oxygen ions, can result in a larger enhancement of hardness than nitrogen. It is interesting to note that at the lowest load (i.e. at the nearest surface region) all the preparative-plus-closing ion implantations increase the hardness relatively higher than other implantations do, as shown by the steeper slopes between the hardnesses with loads of 1 and 3 g for the triply implanted samples (Fig. 1). This fact indicates that the triple ion implantation is more effective in improving nearest-surface-hardness. This is supposedly contributed mainly by the closing implanted ions, which lead to forming hard compounds with either metal elements or even previously implanted nitrogen, as demonstrated by XRD analysis (Fig. 2).

Also, it can be seen from the wear testing results that, similar to the hardness modifications, the triple ion implantation generally reduces wear remarkably, while the wear on either the unimplanted sample or the single and the double N-ion implanted ones is comparatively high. In due

Table 2
Heat treatment procedure of the steel samples

| Preheating | Hardening | Quenching | Tempering |
|---|---|---|---|
| 850°C/5 min | 1050°C/15 min | Oil | 150°C/1+1 h |

Table 3
Ion implantation and mechanical testing results of the SKD11 steel samples[a]

| Sample | Ion | Energy (keV) | Current ($\mu A/cm^2$) | Dose ($10^{17}/cm^2$) | HK ($kg/mm^2$) | Wear rate ($10^{-7}$ $mm^3$/ |
|---|---|---|---|---|---|---|
| S0 | – | 0 | 0 | 0 | 470 | 1.30[b] |
| S1 | $N+N_2+N_2$ | 120-120-90 | 100-200-200 | 2+4+2(N) | 1040 | 0.11 |
| S2-1 | $N+N_2+BF$ | 120-120-90 | 100-200-50 | 2 + 4 + 2(B) | 1410 | 0.10 |
| S2-2 | $N+N_2+BF$ | 120-90-75 | 100-200-30 | 2+4+1(B) | 1046 | 0.11 |
| S3 | $N+N_2+CO_2$ | 120-120-110 | 100-200-100 | 2 + 4 + 2(C) | 1420 | 0.14 |
| S4 | $Ar+N_2+BF$ | 140-120-90 | 200-200-50 | 2+4+2(B) | 1120 | 0.26 |
| S5 | $N_2$ | 120 | 200 | 4 | 795 | 1.30 |
| S6 | $N+N_2$ | 120-120 | 100-200 | 2 + 4 | 895 | 1.26[d] |
| S7 | $N_2+BF$ | 120-90 | 200-50 | 4 + 2(B) | 1200 | 0.19 |

[a] Ion implantations in samples S5, S6 and S7 are for comparison. For the last implantation of multiple ion implantation, when a compound ion species was used, the last dose indicates the atom dose of the element in the (). The microhardness testing condition: 1 g load; the wear testing conditions: WC ball, 500 g load, 4.8 cm/s sliding speed, 10 000 total-rotations.
[b] Obtained only for 700 total-rotations when the friction limit of the tester was reached.
[c] Obtained for 1800 total-rotations when the friction limit was reached.
[d] Obtained for 1900 total-rotations when the limit was reached.

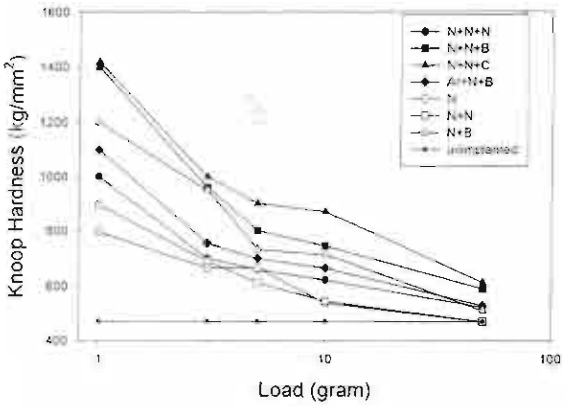


Fig. 1. Microhardness in the Knoop scale as a function of the testing load (1, 3, 5, 10 and 50 g).

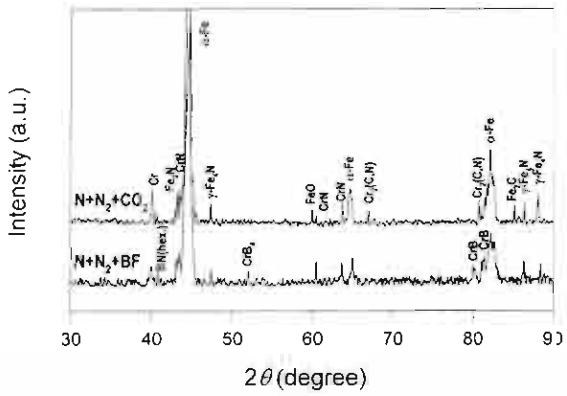


Fig. 2. XRD analyzed results from the $N+N_2+BF$-ion implanted sample and $N+N_2+CO_2$-ion implanted sample. The peaks are only designated once if they have the same positions in both patterns.

succession, the ion species for the preparative implantation being effective on the wear reduction are nitrogen and argon, and the species for the closing implantation are boron, nitrogen, and carbon/oxygen. A close SEM-observation on the surface microstructure of the samples, as shown in Fig. 3, provides some hints. On the surface of the $N+N_2+N_2$ and $N+N_2+BF$ ion implanted samples we can observe an extended large-grained or textured structure whereas on the $N+N_2+CO_2$ and $Ar+N_2+BF$ ion implanted samples we see a much finer and smoother structure. The former microstructure is thought to be related to nitride or boride (as shown in Fig. 2) exhibiting high wear-resistance, while the latter is less helpful to wear resistance due to either brittle oxide for the case of the $N+N_2+CO_2$-ion implanted surface or heavy radiation damage created by Ar-ions for the case of the $Ar+N_2+BF$-ion implanted surface.

The ion-depth-profile analysis, as shown in Fig. 4, leads to a further understanding of the wear

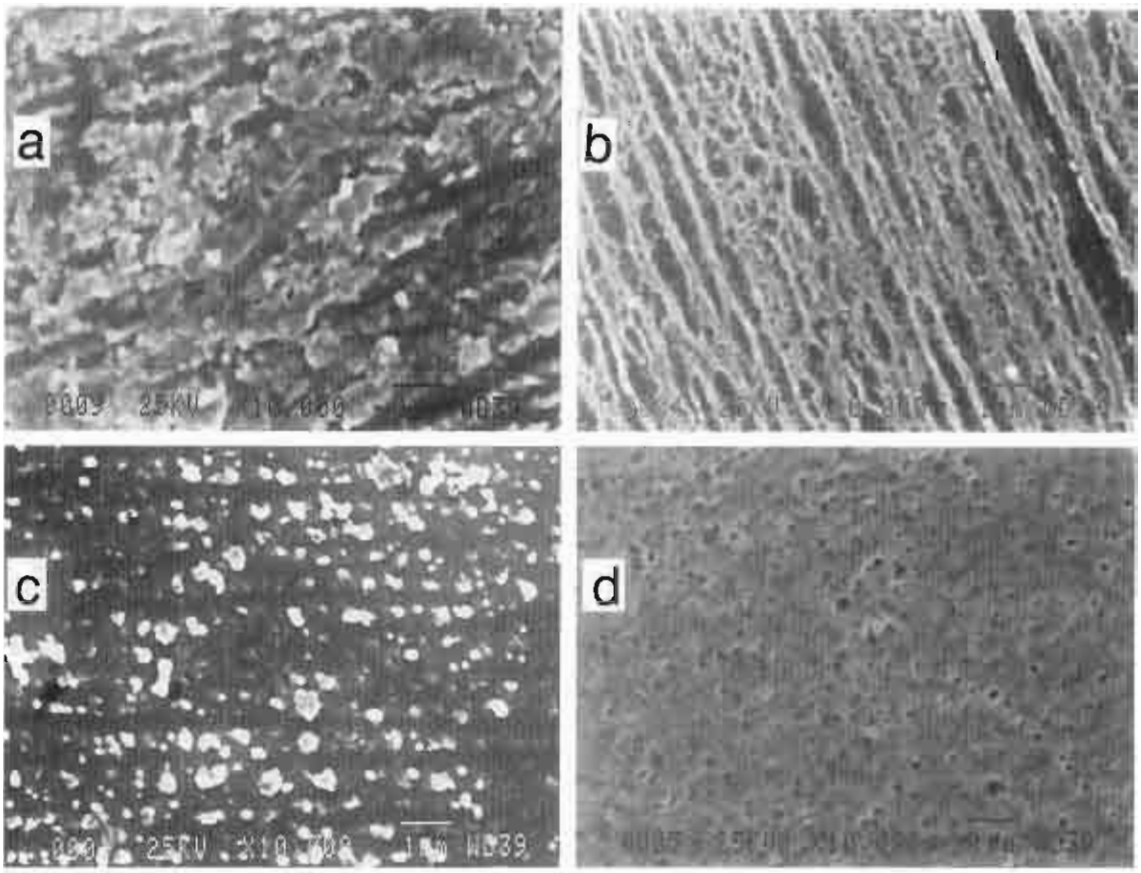


Fig. 3. SEM photographs of the preparative-plus-closing ion-implanted sample surfaces. (a) $N+N_2+N_2$ ion implanted, (b) $N+N_2+BF$ ion implanted, (c) $N+N_2+CO_2$ ion implanted, and (d) $Ar+N_2+BF$ ion implanted. The width of the SEM image is 12 μm.

testing results. The preparative-plus-closing ion implantation generally tends to broaden and deepen the nitrogen distributions. A comparison between the PROFILE-simulated [7] and the measured $N+N_2+N_2$-ion implanted profiles shows that the simulated one (Fig. 4a), which is a sum of three consecutively implanted ion-profiles, ranges only up to a depth of 200 nm while the measured one (Fig. 4b) becomes flat and extends to a depth of more than 600 nm (the depth scale is already converted from the sputtering time). Other profiles display similar behavior. The effect of broadening and deepening ion profiles seems very beneficial in achieving the lasting low wear rates by means of triple ion implantation. It can be seen that the closing B-ion implantation leads partly to the migration of normally implanted N-ions to the B-ion region, as shown in Fig. 4c and e, while the closing $CO_2$-ion implantation causes the normally implanted N-ions to be pushed further into the substrate (Fig. 4d). This fact implies that the implanted boron has a stronger affinity of bonding with the formerly implanted nitrogen [8] than the carbon and oxygen have (correlated with the XRD result, as shown in Fig. 2). Therefore, the $N+N_2+BF$ ion implantation produces a lower wear rate than the $N+N_2+CO_2$ ion implantation. For the case of $Ar+N_2+BF$ ion implantation, it is considered that radiation damage induced by the preparative Ar-ion implantation makes the N-ions migrate more easily to the near surface region, so that the N-ion distribution is shallower (Fig. 4e) than those in other cases. Therefore the low wear rate cannot last and the average wear rate becomes high.

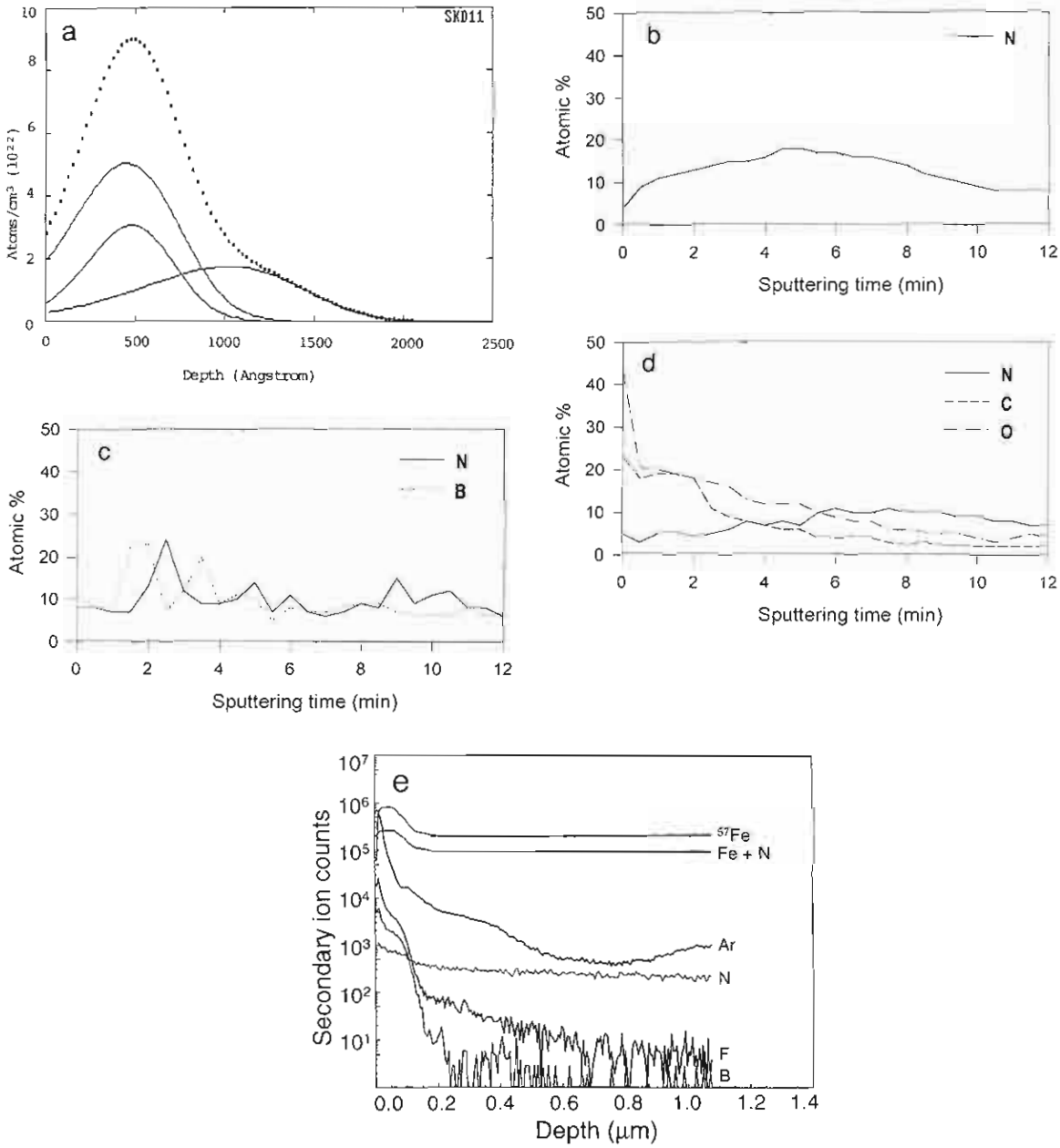


Fig. 4. Analyses of the ion depth profiles. (a) PROFILE-simulated profile for $N+N_2+N_2$ ion implantation with the same parameters as the experimental one's (the dotted curve represents the final profile); (b) AES-analyzed profile for the $N+N_2+N_2$ ion implantation; (c) AES-analyzed profile for the $N+N_2$+BF ion implantation; (d) AES-analyzed profile for the $N+N_2+CO_2$ ion implantation; and (e) SIMS-analyzed profile for the $Ar+N_2$+BF ion implantation.

## 4. Conclusion

The preparative-plus-closing ion implantations result in dramatic increases in surface hardness and wear resistance of the hardened tool steel in comparison with single N-ion implantation and double ion implantation. The degree of improvement depends on the preparative and closing implanting ion species. Nitrogen is better than argon as the preparative implanting species while boron is the best of the closing implanting species. The broadened and deepened N-ion distribution and the formed high-wear-resistant near-surface structure or compound by the preparative-plus-closing ion implantation are considered to be the contributors to this improvement.

## Acknowledgements

We sincerely thank Prof. Jizhong Zhang and Prof. Geoffrey W. Shuy for valuable discussions and assistances in elemental depth profile analysis of our specimens. Two of us, L.D. Yu and T. Sonkaew, thank the National Science and Technology Development Agency for the research fellowships. This work was supported by the Thai Research Fund, the National Metal and Materials Technology Center and the IAEA under Contract RCP 333-F2.301.4.

## References

[1] Y. Kun, L. Heng-De, Z. Xiao-Zhong, T. Jia-He, Nucl. Instr. and Meth. 209/210 (1983) 1063.
[2] G.K. Hubler, F.A. Smidt, Nucl. Instr and Meth. B 7/8 (1985) 151.
[3] C.G. Dodd, G.P. Meeker, S.M. Baumann, J.C. Norberg, K.O. Legg, Nucl. Instr. and Meth. B 7/8 (1985) 219.
[4] M.I. Guseva, Ion Implantation in Nonsemiconductors Materials, Itogi naukii techniki, vol. 5, 1989, p. 5.
[5] L.D. Yu, D. Suwannakachorn, S. Intarasiri, S. Thongtem, D. Boonyawan, P. Vichaisirimongkol, T. Vilaithong, in: J.S. Williams, R.G. Elliman, M.C. Ridgway (Eds.), Proceedings of the 9th International Conference on Ion Beam Modification of Materials (IBMM'95), Canberra, Australia, February 1995, Elsevier, Amsterdam, 1996, p. 982.
[6] Standard Test Method for Wear Testing With a Pin-on-Disk Apparatus, Designation: G99-90, ASTM (June 1990), p. 387.
[7] Profile Code Software, Version 3.20 (1995), Implant Sciences, MA, USA.
[8] L.D. Yu, T. Vilaithong, D. Suwannakachorn, S. Intarasiri, S. Thongtem, Nucl. Instr. and Meth. B 127/128 (1997) 954.

BEAM INTERACTIONS WITH MATERIALS AND ATOMS
Nuclear Instruments and Methods in Physics Research – Section B

# Instructions to Authors

(also accessible via the Elsevier Surfaces and Interfaces Home Page at http://www.elsevier.nl/locate/surfaces)

## Submission of papers

Contributions should be submitted to one of the Editors (see inside front cover). It is suggested that manuscripts originating from Europe, India, The Middle East and Africa be sent to Prof. H.H. Andersen, and from The Americas, The Far East and Australasia, to Dr. L.E. Rehn.
Manuscript and figures should be submitted in duplicate, with one set of good quality figure material for production of the printed figures. If possible, please submit also an electronic version of your contribution on diskette.
Short contributions of less than 1500 words and not subdivided into sections may be published as Letters to the Editor in a shorter time than regular articles as the proofs will normally be corrected by the Publisher.
Submission of a manuscript implies that it is not being considered for publication elsewhere and that the authors have obtained the necessary authority for publication.

## Manuscript preparation

Manuscripts should be written in good English. They should be typed throughout with double line spacing and wide margins on numbered, single column pages. See notes opposite on electronic manuscripts
*Structure*. Please adhere to the following order of presentation: article title, author(s), affiliations, abstract, PACS codes and keywords, main text, acknowledgements, appendices, references, figure captions, tables.
*Corresponding author*. The name, full postal address, telephone and fax numbers and e-mail address of the corresponding author should be given on the first page.
*Classification codes/keywords*. Please supply one to four classification codes (PACS and/or MSC), and up to six keywords of your own choice that describe the content of your article in more detail.
*References* to other publications should be numbered consecutively within square brackets and listed together at the end of the text. In the case of multiple authorship all authors should be listed in the references; only in case of more than ten authors is the first author et al. acceptable.

## Illustrations

The Publisher requires a set of good quality drawings and original photographs to produce the printed figures.
*Line drawings* should be 1.5–3 times larger than the printed size; the height of letters and numbers should, after reduction, fall within the range 1.2–2.4 mm. Do not use too narrow pen widths for machine-plotted graphs. Shaded areas should be shown by means of cross-hatching or a matrix of dots, rather than a continuous grey wash.
*Photographs* should not already be screened (overprinted with the point matrix used by printers). The top side of a photograph should be marked if necessary.
*Colour figures* can be printed in colour when this is essential to the presentation. Authors will be charged for colour reproduction. Further information can be obtained from the Publisher.

## After acceptance

*Notification*. You will be notified by the Editor of the acceptance of your contribution, and invited to send an electronic file of the accepted version to the Publisher, if this is not yet available. After acceptance any correspondence should be addressed to the Publisher at the coordinates below.
*Page proofs* are sent out to the Author in order to check that no undetected errors have arisen in the typesetting or file conversion process. In the proofs only typesetting errors may be corrected. No changes in, or additions to, the accepted paper will be accepted.
*Copyright transfer*. In the course of the production process the authors will be asked to transfer the copyright of the article to the publisher. This transfer will ensure the widest possible dissemination of information.

## Electronic manuscripts

If possible, an electronic version of the manuscript should be submitted on a diskette together with the hard copies of the text and figures, or should be sent (after acceptance) by e-mail or on a diskette to the Publisher. It is the responsibility of the Author to ensure that the electronic version exactly matches the hard copy. No deviations from the version accepted for publication are permissible without the prior and explicit approval by the Editor. Such changes should be clearly indicated on an accompanying print-out of the file.
LaTeX articles and articles prepared with any of the well known word processors can be handled by the Publisher. Further information can be obtained from the Publisher.

## Author benefits

*No page charges*. Publishing in Nuclear Instruments and Methods in Physics Research – Section B is free.
*Free offprints*. The corresponding author will receive 25 offprints free of charge. An offprint order form will be supplied by the publisher for ordering any additional paid offprints.
*Discount*. Contributors to Elsevier Science journals are entitled to a 30% discount on all Elsevier Science books.

## Correspondence with the Publisher

After acceptance of an article any correspondence should be addressed to Elsevier Science B.V., NIM-B, P.O. Box 2759, 1000 CT Amsterdam, The Netherlands
Tel. +31 20 485 2500, fax +31 20 485 2431
e-mail nimb-j@elsevier.nl

North-Holland, an imprint of Elsevier Science

# ภาคผนวก ก11

## Tribological Effects of Oxygen Ion Implantation into Stainless Steel

*P. J. Evans[1], T. Vilaithong[2], L. D. Yu[2], O. R. Monteiro[3], K. M. Yu[3] and I. G. Brown[3]*

[1]Australian Nuclear Science and Technology Organization,
Lucas Heights, NSW 2232, Australia.
[2]Department of Physics, Faculty of Science,
Chiang Mai University, Chiang Mai 50200, Thailand.
[3]Lawrence Berkeley National Laboratory, University of California, Berkeley, Ca 94720.

Accepted for Publication in:

Nuclear Instruments and Methods B

# TRIBOLOGICAL EFFECTS OF OXYGEN ION IMPLANTATION* INTO STAINLESS STEEL

**P.J. Evans**
Australian Nuclear Science and Technology Organization, Lucas Heights, NSW 2234, Australia.

**T. Vilaithong, L.D. Yu**
Department of Physics, Chiang Mai University, Chiang Mai 50200, Thailand.

**O.R. Monteiro, K.M. Yu and I.G. Brown**
Lawrence Berkeley National Laboratory, University of California, Berkeley, CA 94720.

## Abstract

The formation of sub-surface oxide layers by hybrid metal-gas co-implantation into steel and other metals can improve their tribological properties. In this report, we compare the wear and friction performance of previously studied Al+O hybrid implants with that produced by single species oxygen ion ($O^-$) implantation under similar conditions. The substrates were AISI 304L stainless steel disks polished to a final mirror finish using 1 micron diamond paste, and the ion implantation was done using a conventional swept-beam technique at ion energies of 70 or 140 keV and doses of up to $1x10^{17}$ $cm^{-2}$. The wear and friction behaviour of the implanted and unimplanted material was measured with a pin-on-disc tribometer. Here we describe the experimental procedure and results, and discuss the improvement relative to that achieved with surface layers modified by metal-gas co-implantation.

---

P.J. Evans, Physics Division, ANSTO, Private Mail Bag No. 1, Menai, NSW 2234, Australia;

Ph: +61 2 9717 3696; Fax: +61 2 9717 3038; E-mail: pev@ansto.gov.au

*Accepted for publication in Nuclear Instruments and Methods B

PACS codes: 61.72.W, 62.20.Q, 81.40.P, 81.65.L

Keywords: oxygen ion implantation, stainless steel, wear, friction, surface modification.

## INTRODUCTION

Ion implantation has become an accepted method of modifying the tribological properties of metal surfaces. Initial work focused primarily on the use of ions of gaseous elements such as nitrogen and oxygen with significant improvements being observed in many systems. The success of these early studies stimulated research into the effects of other ion species particularly metal ions. While studies on single ion implants have predominated, there has been increasing interest in recent years on the use of dual ion implants [1-4] which have yielded greater enhancements in wear performance. For example, recent studies by Sasaki and co-workers have shown the beneficial effects of Ti+C dual ion implantation into hardened steel (0.95wt%C-3.2wt%Cr)[2,3]. Usually, such dual implants are carried out sequentially, though less frequently simultaneous operation of two ion sources has been used.

Since their inception [5], ion sources based on metal vapour vacuum arcs (MEVVA) [6] have been used extensively for surface modification research. These sources offer a convenient means of generating pulsed, high current ion beams of most elemental and alloyed metals, and some non-metallic species (eg. Si and $LaB_6$). An intrinsic feature of such sources is the solid conducting

cathode, which provides the source of ions for extraction, and this precludes their use for producing ion beams of purely gaseous (or liquid) species. However, a recent innovation in MEVVA source technology has succeeded in adapting them for hybrid metal-gas operation [4, 7-9]. This mode permits the simultaneous implantation of gas and metal ions into a target. A description of the modifications to the source at Lawrence Berkeley National Laboratory together with some early tribological results for various combinations of ions have been presented previously [4,9]. It was found that both wear and friction were reduced in most of the systems studied [4]. Despite these promising early results, some uncertainty remains over the relative concentrations of metal and gaseous ions retained during the implantation process. For

instance, ion beam analysis of the dual implanted surfaces revealed some discrepancies between the measured and expected concentrations of the two ions with the effect being most pronounced for the metal species [4,10]. Possible explanations for this finding were proposed and discussed. Consequently, further investigations were undertaken to provide a better understanding of factors contributing to the observed results. While these investigations have focused on characterisation of the implanted surfaces, we have also performed a number of single ion implants for comparison with the dual implanted materials. This report presents the first results obtained for comparison. In particular, samples of AISI 304L stainless steel have been implanted with oxygen ions under similar conditions to those used for the dual implants. Subsequent pin-on-disc wear testing of these oxygen implants yielded wear and friction data which were then compared with the corresponding results from Al+O dual implants into the same material.

The tribological properties of oxygen implanted steels have been the subject of several previous investigations. Langguth and co-workers [11-13] studied a number of steels, though not AISI 304, implanted with oxygen ions at energies of 50, 100 or 200 keV and doses of 5 or $10x10^{17}$ ions $cm^{-2}$. They reported substantial reductions in wear for many of the implant conditions and steels tested with the best results observed for AISI 52100 at the lowest implant energy of 50 keV [12]. More recently, Rej *et al* [14] have compared conventional and plasma source ion implantation of stainless steel (comparable to AISI 321) with several ion species including oxygen. These authors found no improvement in surface hardness following oxygen implantation to a dose of $1x10^{18}$ ions $cm^{-2}$. Possibly on account of this result, Rej *et al* [14] did not perform wear tests on their oxygen implanted samples. The tribology and microstructure of oxygen implanted AISI 304 stainless steel has been studied by Wei *et al* [15]. Doses in the range $1\text{-}10x10^{17}$ $O_2$ $cm^{-2}$ and an energy of 60 keV were used in their work, which also examined the effect of varying implantation temperatures from 100 - 500°C. For a dose of $4x10^{17}$ $O_2$ $cm^{-2}$, they found the critical load increased with temperature to a maximum of 28 N at 400°C, after which it decreased.

## EXPERIMENTAL

As in our previous study [4], the test pieces were disks of type AISI 304L stainless steel (30 mm diameter x 3 mm thick) diamond polished to a mirror finish. These were implanted with 70 or 140 keV oxygen ions ($O^+$) using a mass-analysed oxygen ion beam. Applied doses were in the range $1x10^{16}$ - $1x10^{17}$ ions $cm^{-2}$ with ion beam currents of 10-12 and 30-35 μA at 70 and 140 keV respectively. The beam was scanned over the target to achieve a uniform implant dose. With all samples, an annular region on the periphery (width ~ 6 mm) was masked to provide a reference area for wear testing. During implantation, target temperatures were monitored with a thermocouple and found to be less than 100 °C. Friction and wear testing was performed on a pin-on-disc tribometer (CSEM) using a 6 mm diameter ruby ball, a load of 2 N and a velocity of 0.2 $ms^{-1}$. No lubrication was used for the friction measurements while ethanol was flowed over the test surface during the wear tests. Wear tracks after 1000 revolutions from both the implanted and masked regions of each test sample were analysed with a profilometer (Tencor Instruments). The oxygen concentrations in the steel test pieces were not determined directly. Rather, small pieces of beryllium were mounted at the centre of each sample during implantation. The oxygen doses in these Be reference samples were then measured by RBS analysis using a 1.95 MeV $He^+$ beam.

## RESULTS AND DISCUSSION

The RBS spectra of two Be samples implanted to a dose of $1x10^{17}$ ions $cm^{-2}$ at energies of 70 and 140 keV are shown in Fig.1. The oxygen doses determined from these and similar spectra for the other implant conditions are tabulated in Table 1. Agreement between the nominal and measured doses is reasonable. The implant doses for the steel substrates can be assumed equal

to those determined for the Be samples provided little or no sputtering occurs with the former. This would appear to be a reasonable assumption under the present implant conditions since previous studies [11–15] on a range of steels, including AISI 304, have reported much higher retained doses at similar energies; results which would only have been possible in the absence of significant sputtering.

Since the implant depth profiles in the steel specimens were not measured directly, T-DYN [16] simulations were performed to estimate the oxygen distributions under present conditions. Initially, such calculations were applied to the implanted Be reference samples in order to permit comparison with the oxygen profiles determined from RBS analysis. The resulting profiles are displayed in Fig. 2. For the highest doses at 70 and 140 keV, these are in fair agreement with the measured profiles of Fig. 1. Applying T-DYN to the implanted steel specimens yielded the distributions in Fig. 3. As found previously with the oxygen implanted Be, the calculated profiles for steel may differ somewhat from the actual ones. However, these differences notwithstanding, simulations of the type presented in Figs. 2 and 3 do provide a qualitative indication of changes in implant distributions resulting from different processing conditions. Thus, the profiles in Fig. 3 clearly show the effect of ion energy on the concentration of oxygen at the surface of the steel specimens for the two energies used in the present study.

Friction measurements were performed on all samples. The largest decrease in friction was observed for the oxygen dose of $1 \times 10^{17}$ ions $cm^{-2}$ implanted at 70 keV. The friction trace for these conditions and the corresponding trace from the masked region on the same sample are plotted in Fig. 4. At the same energy, the medium dose of $6.5 \times 10^{16}$ ions $cm^{-2}$ showed less improvement while the lowest dose sample yielded a trace similar to that of the unimplanted material. A similar trend was observed in the friction traces for the low and medium dose implants at the higher ion energy of 140 keV. However, the highest dose at this energy yielded

a result which was little different from that obtained at the medium dose, suggesting deeper implants are not as effective in improving the properties of the layer closest to the surface.

The profilometer traces of wear tracks on the as-polished and implanted ($O^+$ dose = 6.5 x $10^{16}$ ions $cm^{-2}$ at 70 keV) regions of the same specimen are shown in Fig. 5. The large change produced by oxygen implantation is clearly evident in this data. Similar measurements were performed on all samples wear tested for the present study and the results are plotted in Fig. 6. The ordinate in this figure is the ratio of the wear track cross-sectional area on the as-polished steel to that on the implanted region of the same sample. The values used for determining these ratios were the cross-sectional areas below the baseline defined by the original surface of the sample. The ratios plotted in Fig. 6 are the averages of multiple measurements on each sample at different positions on each wear track.

The present results are in general agreement with those of previous studies which reported improvement in the tribological properties of steels following oxygen implantation under a variety of conditions [11-13, 15]. Of particular note is the work of Langguth *et al* [11, 12] who implanted AISI 52100 steel at energies of 50, 100 and 200 keV and found the largest reduction in wear occurred at 50 keV. This trend is similar to that found herein for AISI 304L steel where samples implanted with $O^+$ ions at 70 keV exhibited less wear than those at 140 keV for all doses studied.

The aim of the present study was to compare the effect of dual metal + oxygen implants to those of oxygen-only on type AISI 304L stainless steel. Previously, we reported the results of wear and friction measurements on a nominal 50:50 Al+O implant into this material [4]. While the oxygen-only implants of the present study produced an improvement in wear performance, the magnitude of the effect was greater for the Al+O implants. For example, the wear track cross-sectional area ratio for the Al+O case was ~10 whereas the best value obtained for oxygen only

was 3.6. Thus, selected metal + gas hybrid implantation is capable of producing superior wear resistance relative to single species oxygen implantation. Similarly, the duration of reduced friction was greater for the dual implant. For the 50:50 Al+O implant, a lower coefficient of friction was maintained for a running distance in excess of 6 m. This is significantly longer than the total running distance to breakthrough of 3.5 m recorded for the sample of Fig. 4, which represented the best result of the oxygen only implants studied. The better friction performance achieved with the Al+O implant showed a similar trend to that of the wear data discussed previously. Together, these findings indicate greater improvements in tribological properties are possible with the hybrid treatment.

## CONCLUSIONS

The implantation of oxygen into AISI 304L stainless steel resulted in reduced wear and a lower coefficient of friction. This behaviour was most pronounced at highest oxygen dose and lowest ion energy of the ranges studied. Comparison of the present data with previously reported results for dual Al+O implants into the same steel indicated the presence of Al leads to a further improvement in tribological performance. This finding is in accordance with earlier studies in which surface properties, enhanced by implantation of a single ion type, were further improved following implantation of a second ion species. Therefore, the implantation of selected combinations of ions appears to offer an attractive alternative to the more conventional single implant method. While a variety of approaches have been used for dual ion implantation, the recently developed hybrid MEVVA ion source provides a convenient means of performing such implantations. Future studies will examine the application of this hybrid source in more detail with particular emphasis on the benefits to be derived from the use of dual ions and the operational conditions producing optimum surface properties.

## ACKNOWLEDGMENTS

The authors gratefully acknowledge support of the Thai Research Fund for work performed at Chiang Mai University, and the U.S. DOE, Office of Energy Research, under Contract No. DE-AC03-76SF00098 for that part carried out at LBNL.

## REFERENCES


1. L.E. Pope, J.A. Knapp and D.M. Follstaedt, Surf. Coat. Technol., **36** (1988) 361.
2. J. Sasaki, K. Hayashi, K. Sugiyama, O. Ichiko and Y. Hashiguchi, Surf. Coat. Technol., **65** (1994) 160.
3. K. Hayashi, J. Sasaki, K. Sugiyama, O. Ichiko, K. Tanaka and Y. Hashiguchi, Surf. Coat. Technol., **65** (1994) 430.
4. E. M. Oks, G. Yushkov, P. J. Evans, A. Oztarhan, I. G. Brown, M. R. Dickinson, F. Liu, R. A. MacGill, O. R. Monteiro and Z. Wang, Nucl. Instr. Meth. **B, 127/128** (1997) 782.
5. I. G. Brown, J. E. Galvin and R. A. MacGill, Appl. Phys. Lett., **47** (1985) 358.
6. I. G. Brown, Rev. Sci. Instrum., **65** (1994) 3061.
7. P. Spädtke, H. Emig, B. H. Wolf and E. Oks, Rev. Sci. Instrum., **65** (1994) 3113.
8. B. H. Wolf, H. Emig, D. M. Rück, P. Spädtke and E. Oks, Nucl. Instr. Meth. **B, 106** (1995) 651.
9. I. G. Brown, A. Anders, S. Anders, M. R. Dickinson, R. A. MacGill and E. M. Oks, Surf. Coat. Technol., **84** (1996) 550.
10. N. Dytlewski, P. J. Evans, I. G. Brown, F. Liu, E. M. Oks and G. Yushkov, Nucl. Instr. Meth. **B, 136-138** (1998) 644.
11. K. Langguth, A. Kluge and H. Ryssel, Nucl. Instr. Meth. **B, 59/60** (1991) 718.
12. K. Langguth, A. Kluge and H. Ryssel, Wear **155** (1992) 343.
13. K. Langguth and H. Ryssel, Tribol. Int. **26** (1993) 121.
14. D.J. Rej, N.V. Gavrilov, D. Emlin, I. Henins, K. Kern, T. Kurennykh, V.N. Mizgulin, C.P. Munson, M. Nastasi, J.T. Scheuer, V. Vykhodets and K.C. Walter, Mat. Res. Symp. Proc. **396** (1996) 661.
15. R. Wei, P.J. Wilbur, O. Ozturk and D.L. Williamson, Surf. Coat. Technol., **51** (1992) 133.
16. J.P. Biersack, S. Berg and C. Nender, Nucl. Instr. Meth. **B, 59/60** (1991) 21.

## FIGURE CAPTIONS

**Figure 1 -** RBS spectra of Be reference samples implanted with a dose of 1 x $10^{17}$ ions $cm^{-2}$ at ion energies of 70 keV (o) and 140 keV (•).

**Figure 2 -** T-DYN profiles for Be implanted with $O^+$ at ion energies of 70 keV (upper) and 140 keV (lower). The relevant doses are as indicated on the plots.

**Figure 3 -** T-DYN profiles for 304L stainless steel implanted with $O^+$ at ion energies of 70 keV (upper) and 140 keV (lower). The relevant doses are as indicated on the plots.

**Figure 4 -** Friction coefficient as a function of distance travelled for as-polished (upper plot, right axis) and implanted (lower plot, left axis) regions of a type 304L stainless steel specimen. In this case, the $O^+$ dose was 1 x $10^{17}$ ions $cm^{-2}$ at 70 keV.

**Figure 5 -** Cross-sectional profiles of wear tracks on implanted (—) and as-polished (- - -) regions of type 304L stainless steel implanted with an $O^+$ dose of 6.5 x $10^{16}$ ions $cm^{-2}$ at 70 keV.

**Figure 6 -** Plot of ratios of wear track cross-sectional areas as a function of implant dose at 70 keV (♦) and 140 keV (■).

**Table 1 - Summary of Implantation Conditions**

| Sample No. | Ion Energy (keV) | Ion Current (μA) | Nominal Dose ($O^+/cm^2$) | Measured Dose ($O^+/cm^2$) |
|---|---|---|---|---|
| 1 | 140 | 30-35 | $1x10^{17}$ | $1.0x10^{17}$ |
| 2 | 140 | 30-35 | $5x10^{16}$ | $6.0x10^{16}$ |
| 3 | 140 | 30-35 | $1x10^{16}$ | - |
| 4 | 70 | 10-12 | $1x10^{17}$ | $1x10^{17}$ |
| 5 | 70 | 10-12 | $5x10^{16}$ | $6.5x10^{16}$ |
| 6 | 70 | 10-12 | $1x10^{16}$ | $1.0x10^{16}$ |

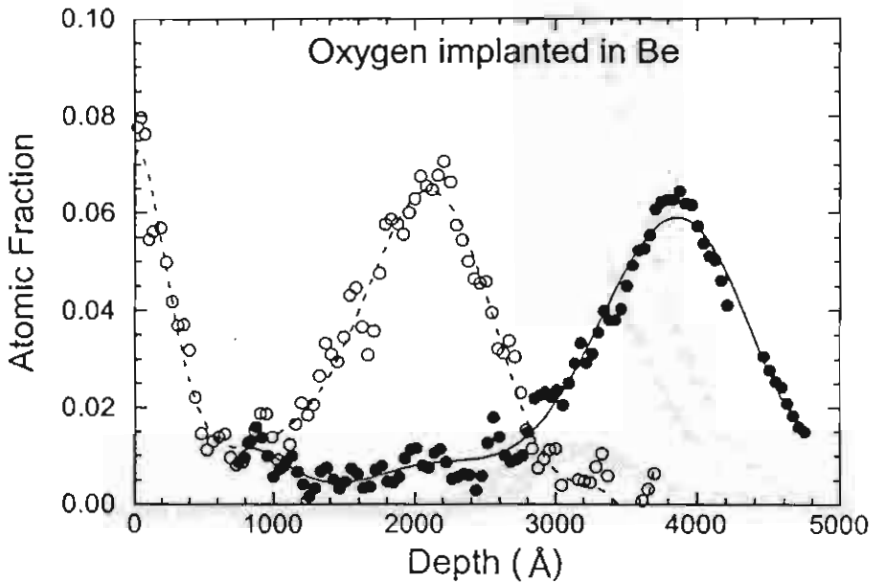
Oxygen implanted in Be
Atomic Fraction
0.10
0.08
0.06
0.04
0.02
0.00
0
1000
2000
3000
4000
5000
Depth ( Å)

Fig.1

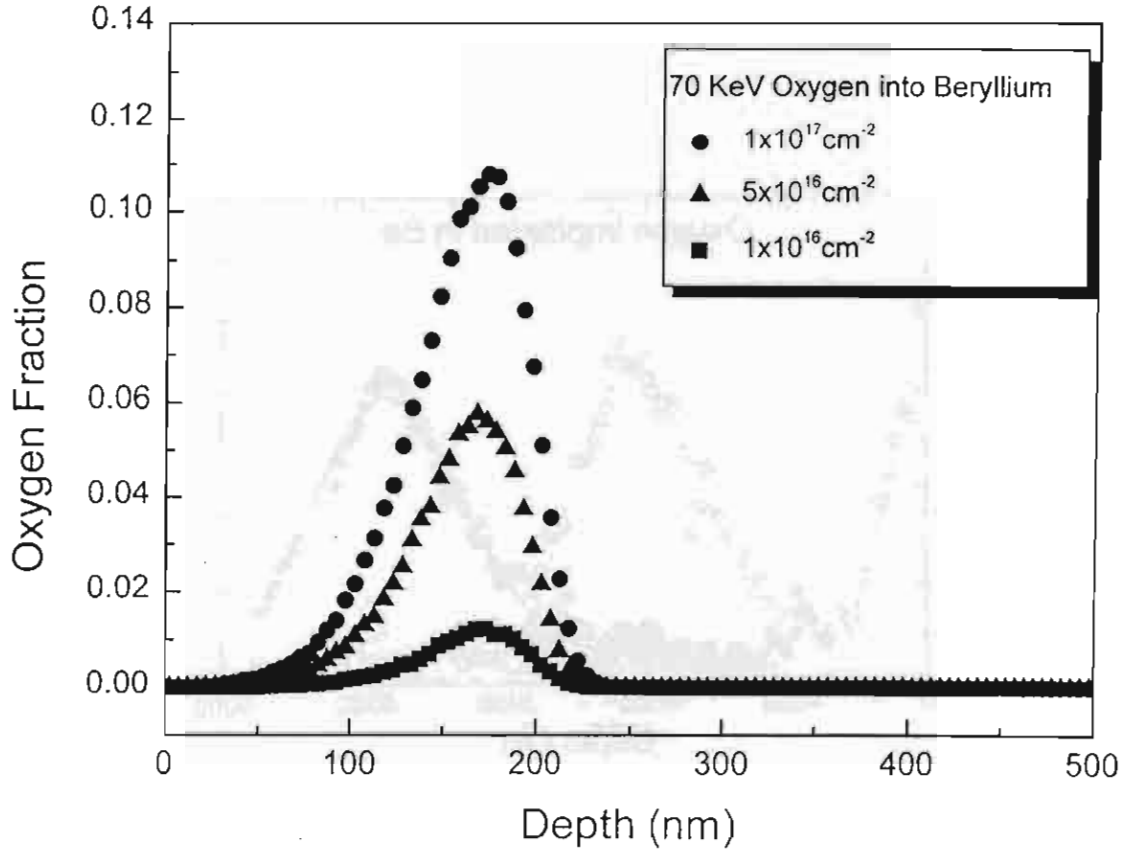
70 KeV Oxygen into Beryllium
1x10^17cm^-2
5x10^16cm^-2
1x10^16cm^-2
Oxygen Fraction
Depth (nm)
0.14
0.12
0.10
0.08
0.06
0.04
0.02
0.00
0
100
200
300
400
500

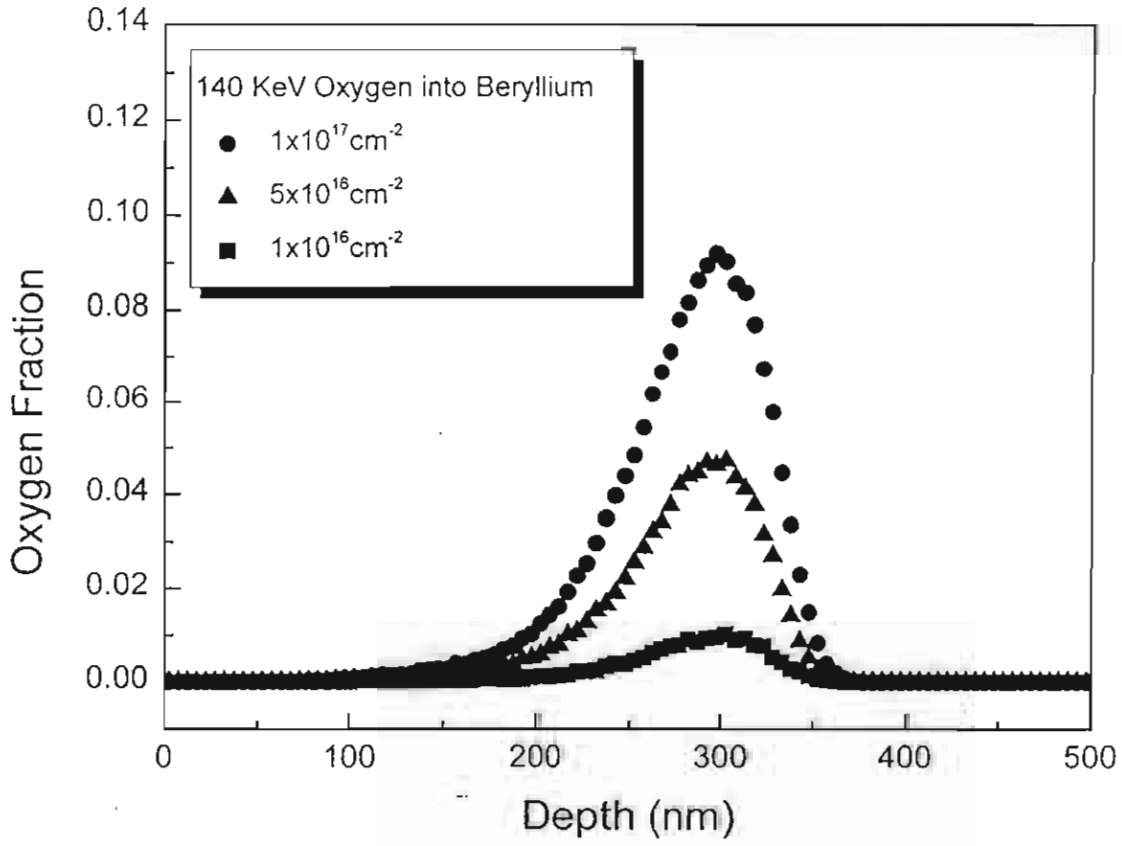
140 KeV Oxygen into Beryllium
1x10^17cm^-2
5x10^16cm^-2
1x10^16cm^-2
Oxygen Fraction
Depth (nm)
0.14
0.12
0.10
0.08
0.06
0.04
0.02
0.00
0
100
200
300
400
500

Fig.2

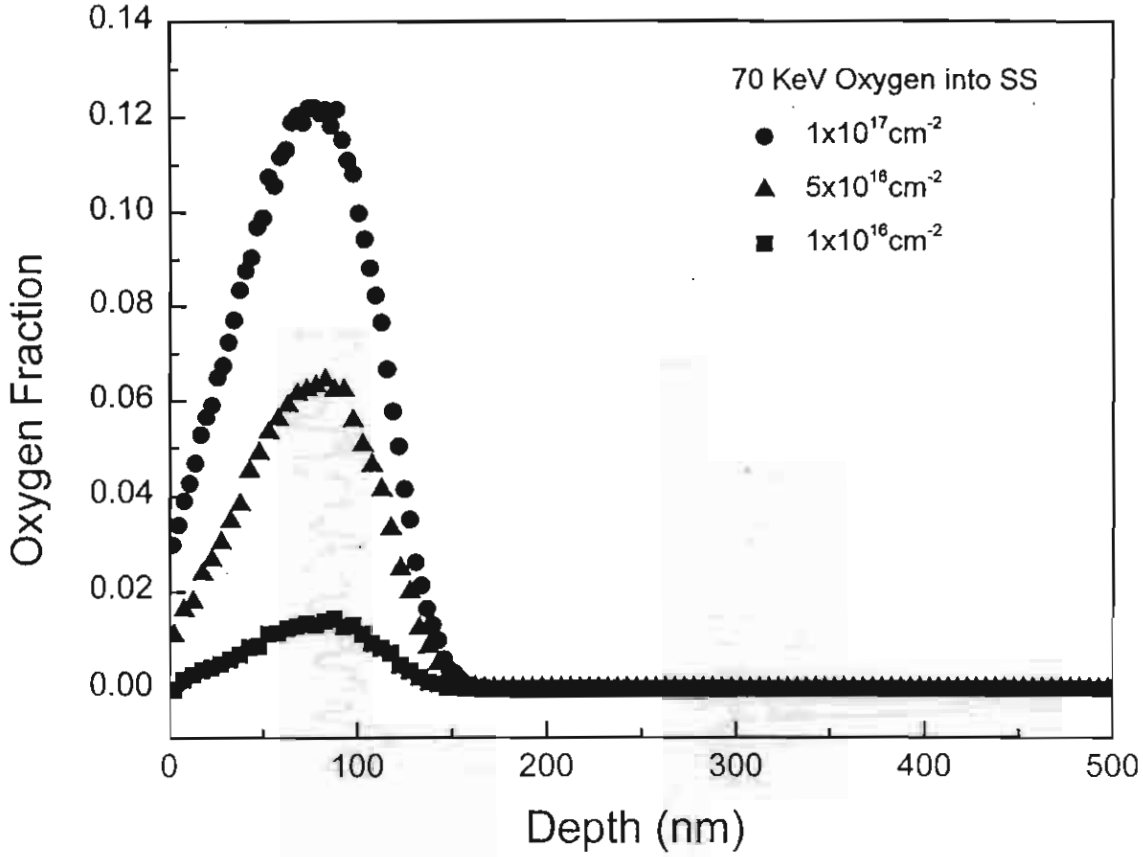
70 KeV Oxygen into SS
1x10^17cm^-2
5x10^16cm^-2
1x10^16cm^-2
Oxygen Fraction
Depth (nm)
0.14
0.12
0.10
0.08
0.06
0.04
0.02
0.00
0
100
200
300
400
500

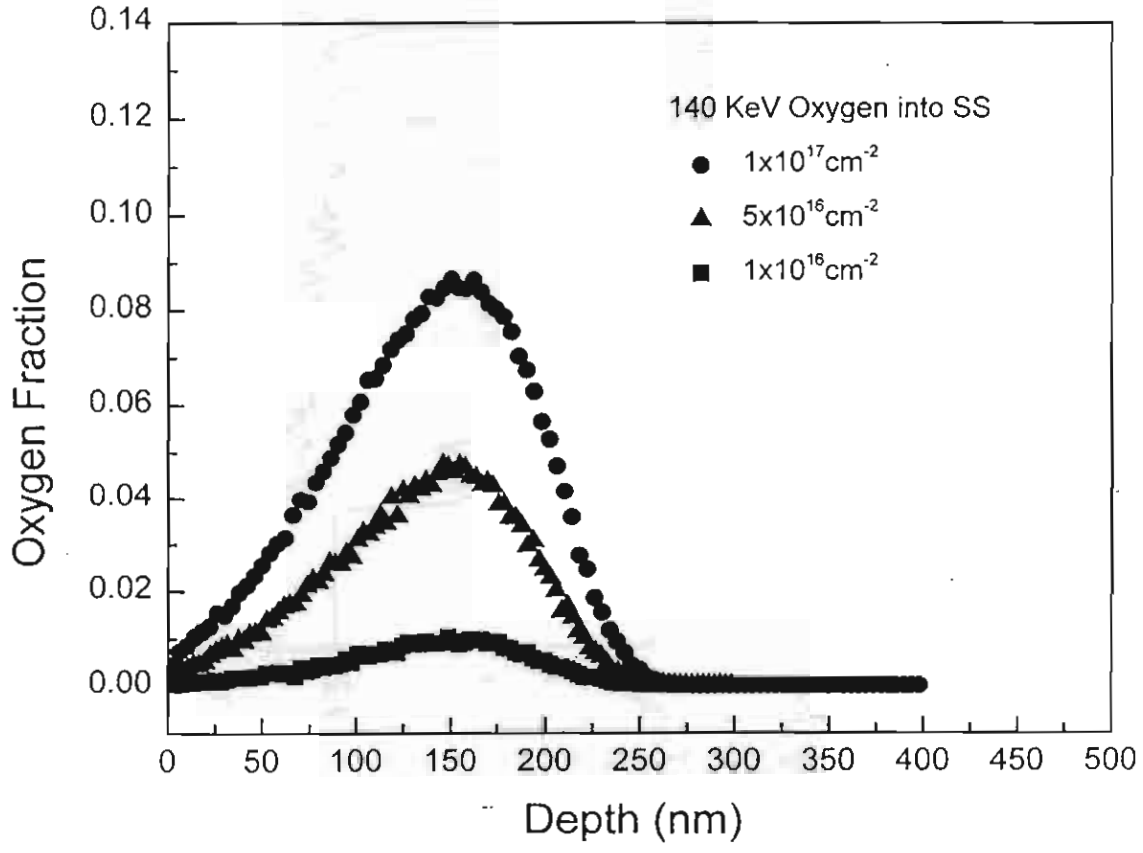
140 KeV Oxygen into SS
1x10^17cm^-2
5x10^16cm^-2
1x10^16cm^-2
Oxygen Fraction
Depth (nm)
0.14
0.12
0.10
0.08
0.06
0.04
0.02
0.00
0
50
100
150
200
250
300
350
400
450
500

Fig.3

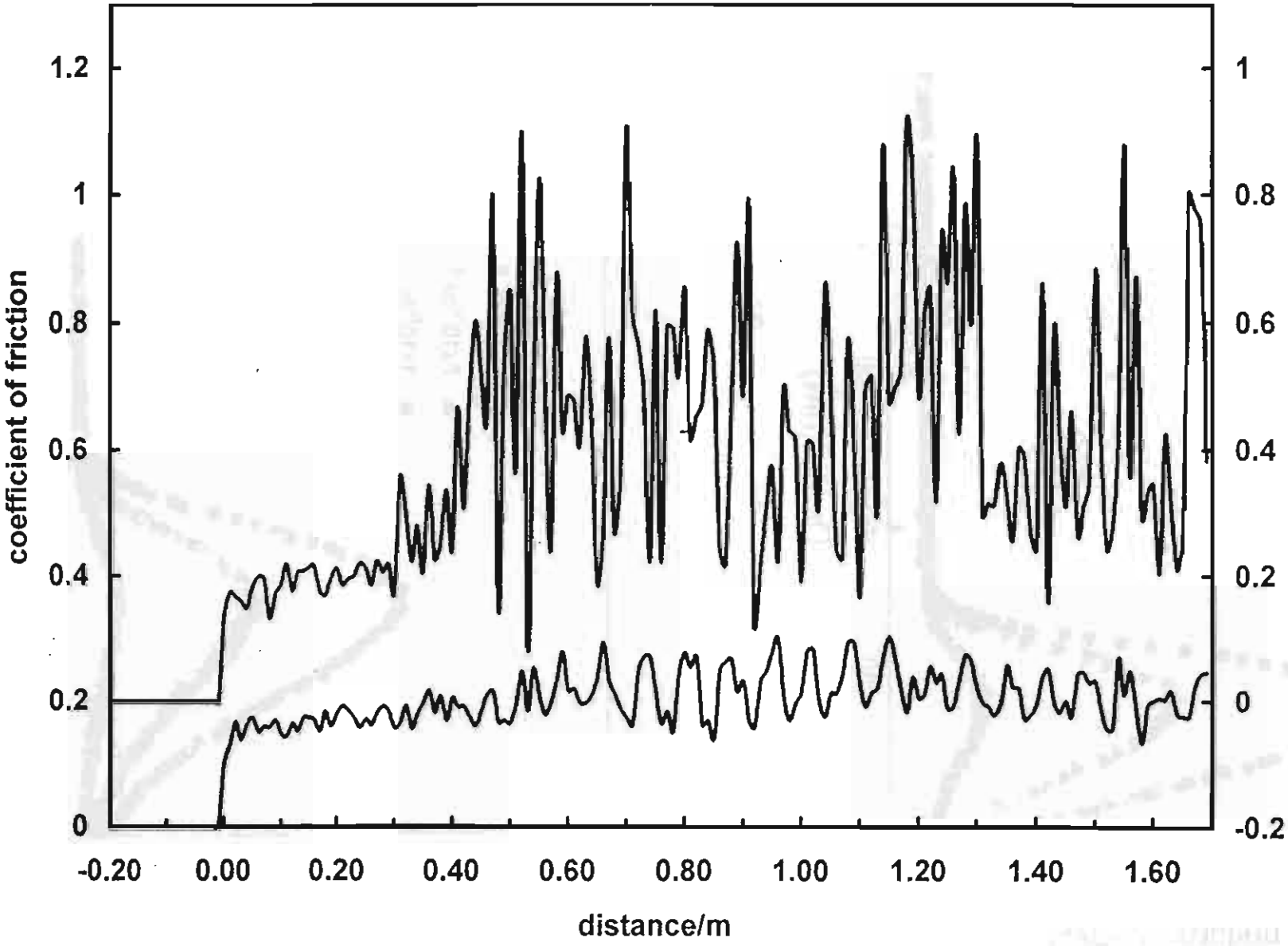
coefficient of friction
1.2
1
0.8
0.6
0.4
0.2
0
1
0.8
0.6
0.4
0.2
0
-0.2
-0.20
0.00
0.20
0.40
0.60
0.80
1.00
1.20
1.40
1.60
distance/m

Fig.4

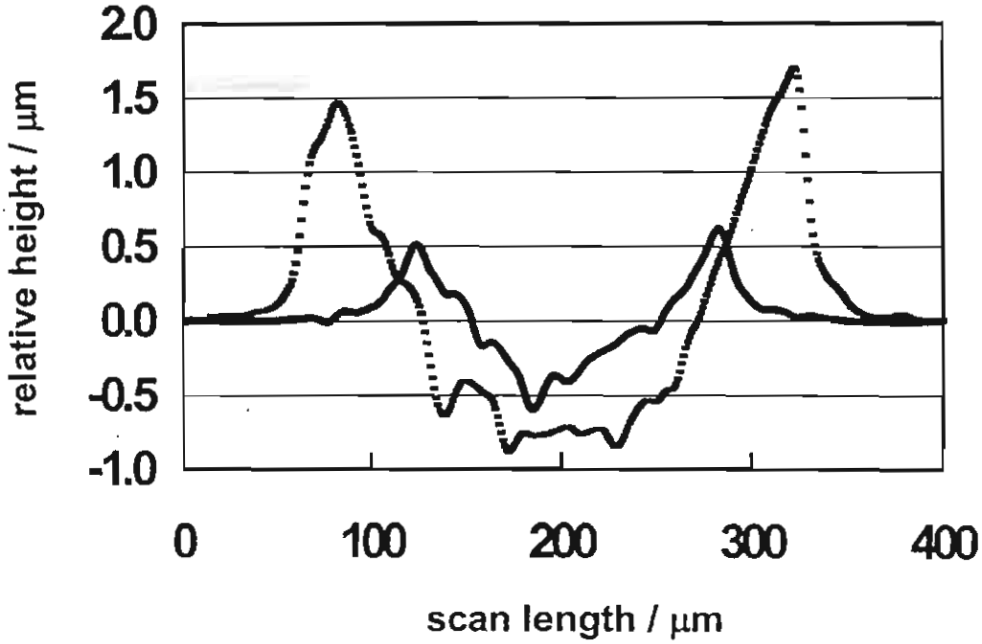
2.0
1.5
1.0
0.5
0.0
-0.5
-1.0
relative height / µm
0
100
200
300
400
scan length / µm

Fig. 5

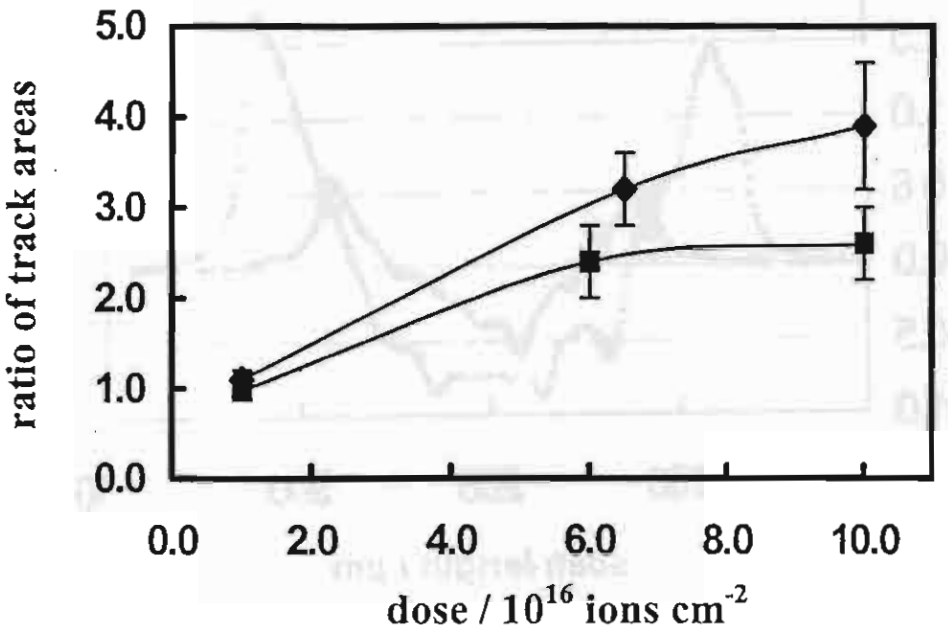
ratio of track areas
5.0
4.0
3.0
2.0
1.0
0.0
0.0
2.0
4.0
6.0
8.0
10.0
dose / 10^16 ions cm^-2

Fig.6

# ภาคผนวก ก12

## Modification of Tribology and High-Temperature Behavior of Ti-47Al Intermetallic Alloy Nitrided by N-Ion Implantation

*L. D. Yu[1], S. Thongtem[2], T. Vilaithong[2] and M. J. McNallan[3]*

[1]Institute for Science and Technology Research and Development,
Chiang Mai University, Chiang Mai 50200, Thailand.
[2]Department of Physics, Faculty of Science,
Chiang Mai University, Chiang Mai 50200, Thailand.
[3]CME Department, University of Illinois at Chicago,
842 W. Taylor St., Chicago, IL 60607-7022, USA.

Accepted for Publication in:

Surface and Coatings Technology.

# Modification of Tribology and High-Temperature Behavior of Ti-47Al Intermetallic Alloy Nitrided by N-Ion Implantation*

L.D. Yu, Institute for Science and Technology Research and Development.
P.O.Box 111, Chiang Mai University. Chiang Mai 50200, Thailand
S. Thongtem. T. Vilaithong. Department of Physics, Faculty of Science.
Chiang Mai University. Chiang Mai 50200. Thailand
M.J. McNallan, CME Department. University of Illinois at Chicago.
842 W. Taylor St.. Chicago. IL 60607-7022. USA

## Abstract

N-ion implantation in Ti-47Al-2Nb-2Cr intermetallic alloy has been investigated for surface nitriding treatment to modify tribology and high-temperature oxidation properties of the material. The alloy samples were implanted using either normal(medium)-current or high-current $N_2$-ion beams at an energy of 140 keV to doses of $4 \times 10^{17} - 4 \times 10^{18}$ions/cm$^2$. Post-annealing was performed to the ion-beam-treated samples at temperatures of 200°C and 300°C for different periods (24 - 240 hours). The treated samples underwent tests of microhardness. tribology and high-temperature oxidation. The results show that N-ion implantation and post-annealing improve surface hardness in all cases. wear resistance in the case of high-current and high-dose ion implantation. and high-temperature oxidation behavior in the early testing stage. N-ion implantation particularly with high beam-current and high ion-dose without post-annealing results in the best modification of tribology. XRD analyses indicate that the formation of metal nitride and oxide is supposed to be responsible for the modification of the relevant properties. The ion implantation compared with the gas-nitriding technique has some advantages and shortcomings.

*Accepted for publication in Surface and Coatings Technology

# 1 Introduction

Ti-Al intermetallic alloys have long attracted materials engineers' interests for their special mechanical and chemical properties [1,2] and their potential tribology and high-temperature applications such as engine valves [3,4]. Among the various Al-contents of the alloys, an alloy possessing an intermetallic phase with a narrow Al-content range around 47 at.% has emerged and been intensively studied [5,6]. A traditional technique of modifying the Ti-Al alloy is gas-nitriding [4]. Since ion implantation technique was developed ion beam nitriding has been attempted to improve the physical and chemical properties of the alloys [3]. We describe here our work employing N-ion implantation under proper implantation and post-annealing conditions as a nitriding means for modification of tribology and high-temperature oxidation of the specific intermetallic alloy.

# 2 Experimental

## 2.1 Processing

Samples of HIPed (Hot Isostatic Pressed) Ti-47Al-2Nb-2Cr intermetallic alloy named MJ12 (Howmet, MI, USA) were cut by a diamond saw from a raw bar into 20 mm diameter and 2 mm thick disks. The sample surfaces were polished by alumina powder to a final finish of 0.3-$\mu$m.

N-ion implantation into the alloy samples consisting of two groups were carried out at low current and dose using an analyzed heavy ion implantation facility and at high current and dose using a non-analyzed high-current N-ion implanter in the Ion Beam Technology Center, Chiang Mai University [7]. Table 1 lists the ion implantation conditions. During implantation, we deliberately employed no target cooling, and the temperatures of the target surface were estimated to be about 100°C for the lower-current implantation and a few hundred °C for the higher-current implantation. The working pressures inside the target chambers were kept in the range between $10^{-4} - 10^{-3}$ Pa.

After ion implantation the samples were annealed step by step in flowing air at temperatures of 200°C to 300°C for various periods as shown in Table 2.

### 2.2 Testing

Hardness testing was performed using an advanced Digital Microhardness Tester on the samples after each step of annealing. A Knoop hardness testing indenter with a load of 5 g was applied to various positions at random on each sample surface. Average values and standard deviations of the Knoop hardness number HK (in kg/mm$^2$) for each sample were automatically calculated and printed out by the tester software.

Tribology testing was performed on the samples after the annealing was completed in a laboratory air atmospheric environment using a pin-on-disk tribometer where the sample was the rotating disk and a ball with a proper load was fixed to slide on the disk. The ball material was WC ($r$ = 3.175mm). The load was 250 g or 50 g, the sliding speed was 4.8 cm/s and the total rotations were 10000.

Oxidation test was performed using a high-temperature gas flow testing system [8]. The samples were hung in a refractory tube, where normal air at 1200 K flowed through at a rate of 8 cm$^3$/s. The test lasted for a total of 10 hours. The samples were regularly taken out during the testing period for measuring the mass change by a sensitive digital balance.

### 2.3 Analysis

XRD, using a Cu target ($K_\alpha$) at 30 kV with a current of 30 nA, was performed on the samples for identification of compound formation. An image microscope was used to observe the sample surface microstructure.

## 3 Results

**Microhardness:** Figure 1 shows changes in the surface microhardness owing to ion implantation and post-annealing. It is clear that surface hardness has been improved by the treatments. However, the change in the hardness with annealing step for the low-current ion-beam implanted alloy is much different from that for the high-current beam implanted one.

**Tribology:** Table 3 lists the tribology testing results. The data from either the higher-load or the lower-load tested samples behave similarly. For low-current and low-dose ion implanted

samples the wear rates and friction coefficients do not have significant changes whereas the as-implanted data show better improvements than the annealed one for the high-current and high-dose ion implanted samples.

**High-temperature oxidation:** The rate of mass change at the high temperature as a function of the testing time for differently processed samples is shown in Figure 2. It is seen that in the first 2-hour period of the total testing time the mass-increase rates of all the ion-implanted samples are lower than that of the unimplanted one. Then after, the oxidation rate of the unimplanted one becomes saturated.

**XRD:** Figure 3 shows the XRD patterns from the ion-implanted and annealed samples compared with the pattern from the virgin sample. Some nitride and oxide such as $Ti_2AlN$, $Nb_3Al_2N$, TiO and $Ti_3O_5$ formed after ion implantation, especially, after further annealing. A comparison between the high-current and low-current ion implanted results indicates that the $Ti_2AlN$ and TiO peaks of the former case are more pronounced than those of the latter case.

## 4 Discussion

**Hardness:** For the case of the low-current ion beam implanted samples, the decrease in hardness in the preliminary annealing stage is thought to be caused by annealing-relaxation of the ion-implantation-induced surface compression tension, which originally contributes to the surface hardness increase [9]. With an increase in nitride and oxide formation by the annealing process, the surface becomes harder and harder up to an almost constant level. For the high-current and high-dose ion implanted alloy, rich nitrogen as well as the higher annealing temperature makes the nitriding dominant in the process [10,11], so that the hardness increases with the annealing almost linearly.

**Tribology:** Surface microstructure analysis by image microscopy indicates different structures formed in the as-implanted surface and the post-annealed surface as shown in Figure 4. The martensite-like structure of the as-implanted surface may play a resistive role to wear. Although the nitride and oxide formed due to annealing results in a high hardness, the hard

debrises falling off from the nitrided surface during wear might severely abrade and harm the alloy surface. Therefore, the annealed surface was worn much more. This interpretation is supported by the microscopic surface observation on the wear tracks of the wear-tested samples as shown in Figure 5, where more abrasive wearing grooves are seen in the track of the annealed surface than the unannealed one. In fact, modification of wear resistance is affected by factors involving both surface structure and composition [12] such as nitride and oxide formation which compromise for an optimum improvement in the resistance.

**High-temperature oxidation:** The result indicates that the nitride formed due to ion implantation does reduce oxidation. If the oxidation behavior of two different surfaces is simplified as shown by an insert on the top-left hand corner of Figure 2, in which one characterized by a typical parabolic curve and the other by a straight line with a lower slope at the primary stage, a conclusion obviously drawn from such behavior is that the latter has an intrinsic oxidation rate lower than the former does. Because the well-known parabolic oxidation behavior [13] is caused by intense oxidation in the first stage then followed by protection owing to an increasingly accumulated oxide. The oxidation tending to moderation in the parabolic behavior is simply due to the oxide and not the material itself. Therefore, it is said that the oxidation of the ion-implanted samples is intrinsically reduced. Because of lower oxidation rates the ion-implanted samples were oxidized slowly and could not accumulate sufficient oxide to protect their surfaces from being further oxidized, and hence, their oxidation behaves nearly linearly with time. The phenomenon exhibited at the later testing stage is consistent with the result reported in [3] which, however, did not notice some details occurring in the early testing stage. The oxide protection role can be understood by the fact that only the unimplanted data obey the parabolic oxidation law quite well. The formed oxide virtually protected the surface in any case so that the implanted data still show the parabolic behavior, but very obtusely. The protective role of the oxide can be further demonstrated by the fact that the data from the annealed samples are generally lower than the data from the unannealed ones in the case of high-current and high-dose implantation, as shown in the figure, because the annealing already easily created oxide on the heavily ion-irradiated surface [14] before the oxidation test. For the low-current ion implantation the wear rate data from both unannealed and annealed samples are not noticeably different as

the ion-irradiation damage on the surface are not heavy.

## 5 Conclusion

The Ti-47Al intermetallic alloy nitrided by N-ion implantation and post-annealing increases its surface microhardness under various ion implantation conditions particularly with increasing of the beam current, ion dose and annealing time. The high-current, high-dose ion implantation without post-annealing is found to be most beneficial in improving tribological properties. The high-temperature oxidation rates are reduced in the early testing stage for the alloy in all cases of N-ion implantation. The alloy is indeed nitrided by the ion beam processing assisted by the annealing, and the formed metal nitride and oxide are shown to be responsible for the modification of the relevant properties.

Compared with gas-nitriding [4], the high-current and high-dose N-ion implantation without post-annealing to achieve the similar modification of the alloy has the advantages of having much short processing time, being "cold" treatment and preserving original surface morphology. The shortcomings of having thin modified layers and lower improvement in tribology.

## 6 Acknowledgments

We wish to thank Howmet Corp., MI, USA, for supplying the researched material. The technical assistance of G. Rujijanagul and T. Sonkaew in XRD measurement is gratefully acknowledged. This work was supported by the National Metal and Materials Technology Center and the Thailand Research Fund.

## References


[1] H.A. Lipsitt, D. Shechtman and R.E. Schafrik, Met. Trans. 6A(1975)1991.

[2] T. Kawabata, T. Kanai and O. Izumi, Acta Met. 33(1985)1355.

[3] X. Wang, Y. Yang, X. Liu, S. Zou, S. Taniguchi, K. Takahashi and M. Iwaki, Nucl. Instr. and Meth. B80/81(1993)250-253.

[4] S. Thongtem, T. Thongtem, M.J. McNallan, L.D. Yu, J. of Mat. Proc. & Manuf. Sci., Vol.6, (Jan. 1999)185.

[5] J.D. Sunderkotter, H.J. Schmutzler, V.A.C. Haanappel, R. Hofman, W. Glatz, H. Clemens and M.F. Stroonsnijder, Intermetallics 5:7(Nov. 1997)525-534.

[6] D.Y. Seo, C.H. Wu and T.R. Bieler, Materials Science and Engineering A - Structural Materials Properties, Microstructure and Processing 240(Dec. 1997)450-456.

[7] T. Vilaithong, D. Suwannakachorn, B. Yotsombat, D. Boonyawan, L.D. Yu, S. Davydov, M.W. Rhodes, S. Intarasiri, P. Suanpoot, R. Charoennugul, P. Vichaisirimongkol, S. Aumkaew and V. A-no, ASEAN Journal on Science and Technology for Development 14(2)(1997)87-102.

[8] L.D.Yu, S.Thongtem, D.Suwannakachorn and T.Vilaithong, Proceedings of the International Conference on Materials Technology — Recent Developments and Future Potential, Chiang Mai, Thailand, January 1997, p.308.

[9] W.D. Shi, X.Y. Wen, J.H. Liu, C.S. Ren, Z.H. Long, G.B. Zhang, Z.X. Gong, Y.N. Wang and T. Zhang, Nucl. Instr. and Meth. B80/81(1993)229.

[10] R.Wei, P.J.Wilbur, W.S.Sampath, D.L.Williamson and L.Wang, Lubrication Engineering (April 1991)326.

[11] Arjen M. Vredenberg, Ion Beam Synthesis of Nitride Layers in Iron, Ph.D. thesis, FOM-Instituut voor Atoom- en Molecuulfysica, Kruislaan 407, 1098 SJ Amsterdam, Netherlands.

[12] G. Dearnaley, Nucl. Instr. and Meth. B50(1990)358-367.

[13] M.G. Fontana and Norbert D. Greene, Corrosion Engineering, 2nd edition, McGraw-Hill Book Company (New York, 1978)pp.355-357.

[14] J.K.Hirvonen and C.R.Clayton, in: Surface Modification and Alloying by Laser, Ion and Electron Beams, eds., J.M.Poate, G.Foti and D.C.Jacobson, (Plenum Press, 1983)p.422.

Table 1. Ion implantation conditions. During implantation the analyzed beam (l-c: low current) was swept on the target while the non-analyzed beam (h-c: high current) was fixed.

| Ion beam type | Ion | Energy (keV) | Beam current ($\mu$A) | Dose (N-atoms/cm$^2$) |
|---|---|---|---|---|
| analyzed beam (l-c) | $N_2^+$ | 140 | 60 | $4 \times 10^{17}$ |
| non-analyzed beam (h-c) | $N^+ + N_2^+$ | 140 | 500 | $4 \times 10^{18}$ |

Table 2. Annealing steps of the samples implanted by the low-current ion beam or the high-current ion beam.

| Ion beam type | Low current | | | | | | | High current | |
|---|---|---|---|---|---|---|---|---|---|
| Annealing step | 1 | 2 | 3 | 4 | 5 | 6 | 7 | 1 | 2 |
| Temperature (°C) | 200 | 200 | 200 | 200 | 200 | 300 | 300 | 300 | 300 |
| Time (hours) | 24 | 24 | 24 | 48 | 48 | 24 | 24 | 24 | 24 |
| Total time (hours) | 24 | 48 | 72 | 120 | 168 | 192 | 216 | 24 | 48 |

**Table 3.** Microhardness and tribology testing results. HK: Knoop hardness number; "annealed": after the total annealing steps were completed (the annealing steps refer to Table 2). The numbers (1) and (2) represent the load conditions under 250 g and 50 g respectively. The friction coefficients are the mean values for the total tested sliding distance.

| Sample type | Hardness HK($kg/mm^2$) | Wear rate ($10^{-6}mm^2$) | Friction coefficient |
|---|---|---|---|
| virgin | 330 | (1) 2.15; (2) 0.80 | (1) 0.7; (2) 1.2 |
| low-current as-implanted | 656 | (1) 2.14; (2) 0.77 | (1) 0.7; (2) 1.2 |
| low-current implanted & annealed | 841 | (1) 1.59; (2) 0.80 | (1) 0.7; (2) 1.0 |
| high-current as-implanted | 806 | (1) 0.36; (2) 0.22 | (1) 0.7; (2) 0.6 |
| high-current implanted & annealed | 1291 | (1) 1.39; (2) 0.70 | (1) 0.6; (2) 0.9 |

## Figure Captions

**Figure 1.** Microhardness of the N-ion implanted samples compared with that of the unimplanted. The testing load is 5 g. The Annealing Step refers to Table 2; the data for Step 0 are from the as-implanted samples.

**Figure 2.** High-temperature oxidation rate as a function of the testing time. The oxidation rate is defined as the ratio of the mass change of the sample during a given test period and the processed surface area on the sample. The insert shows a simplified oxidation behavior.

**Figure 3.** XRD patterns of the processed samples compared with the unprocessed one.

**Figure 4.** Image microscopic photographs of (a) the as-implanted surfaces and (b) the post-annealed surfaces. The upper ones are treated by the low-current ion beams and the lower ones by the high-current ion beams.

**Figure 5.** Wear tracks of (a) the as-implanted surface and (b) the post-annealed surface implanted with high-current and high-dose N-ions.

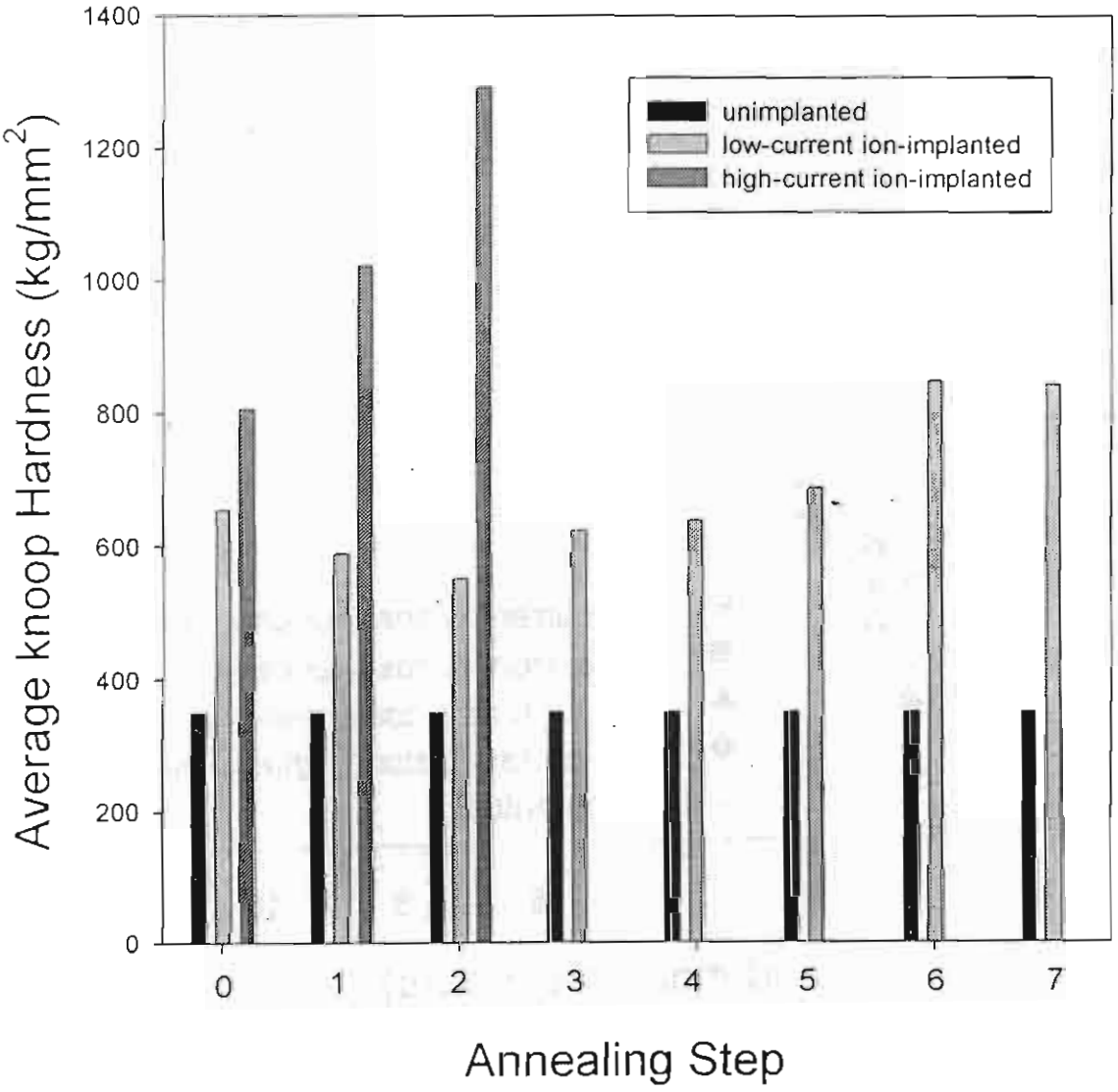
1400
1200
1000
800
600
400
200
0
Average knoop Hardness (kg/mm$^2$)
unimplanted
low-current ion-implanted
high-current ion-implanted
0
1
2
3
4
5
6
7
Annealing Step

Fig. 1

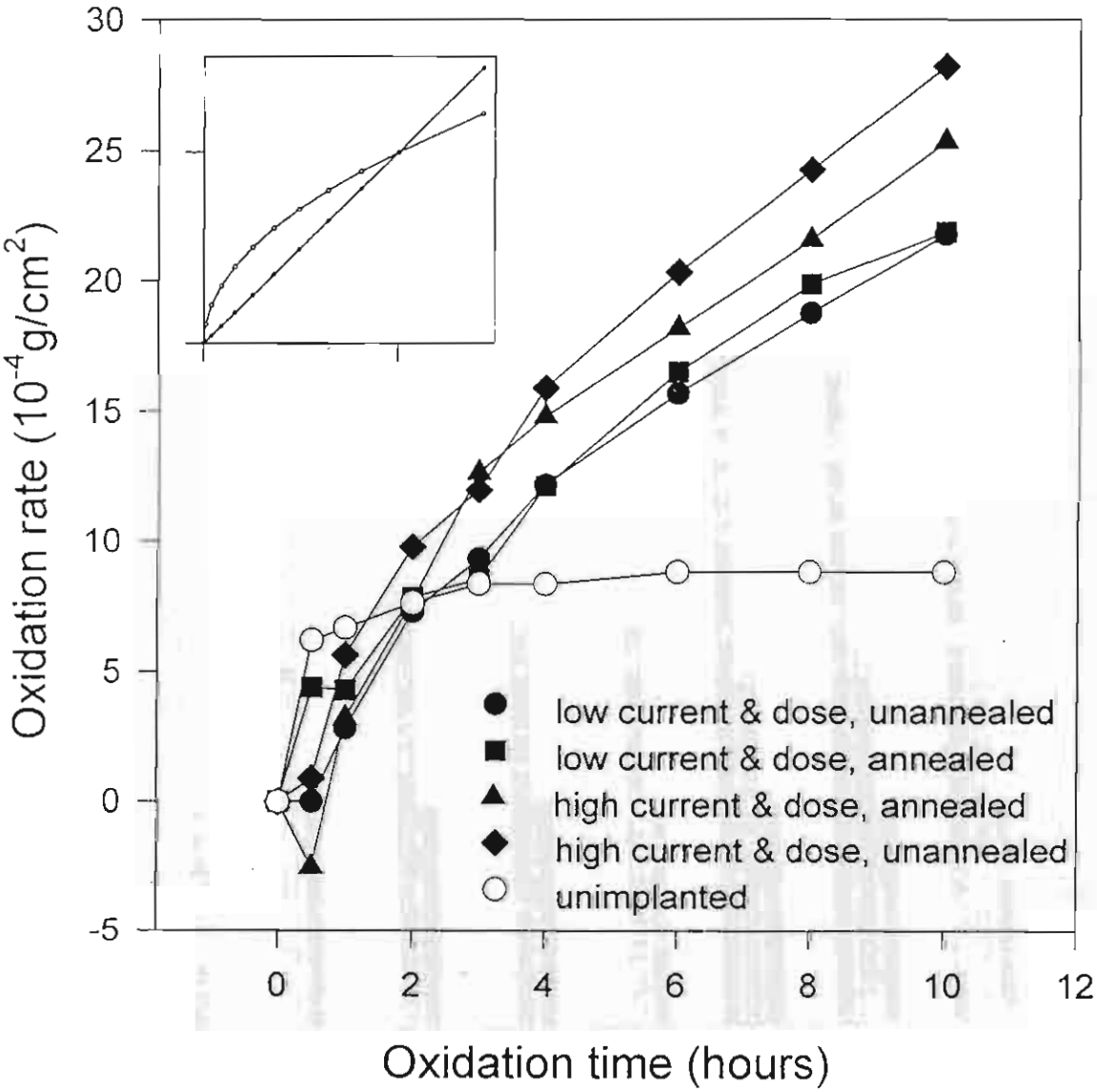
Oxidation rate ($10^{-4}$g/cm$^2$)
30
25
20
15
10
5
0
-5
0
2
4
6
8
10
12
Oxidation time (hours)
low current & dose, unannealed
low current & dose, annealed
high current & dose, annealed
high current & dose, unannealed
unimplanted

Fig. 2

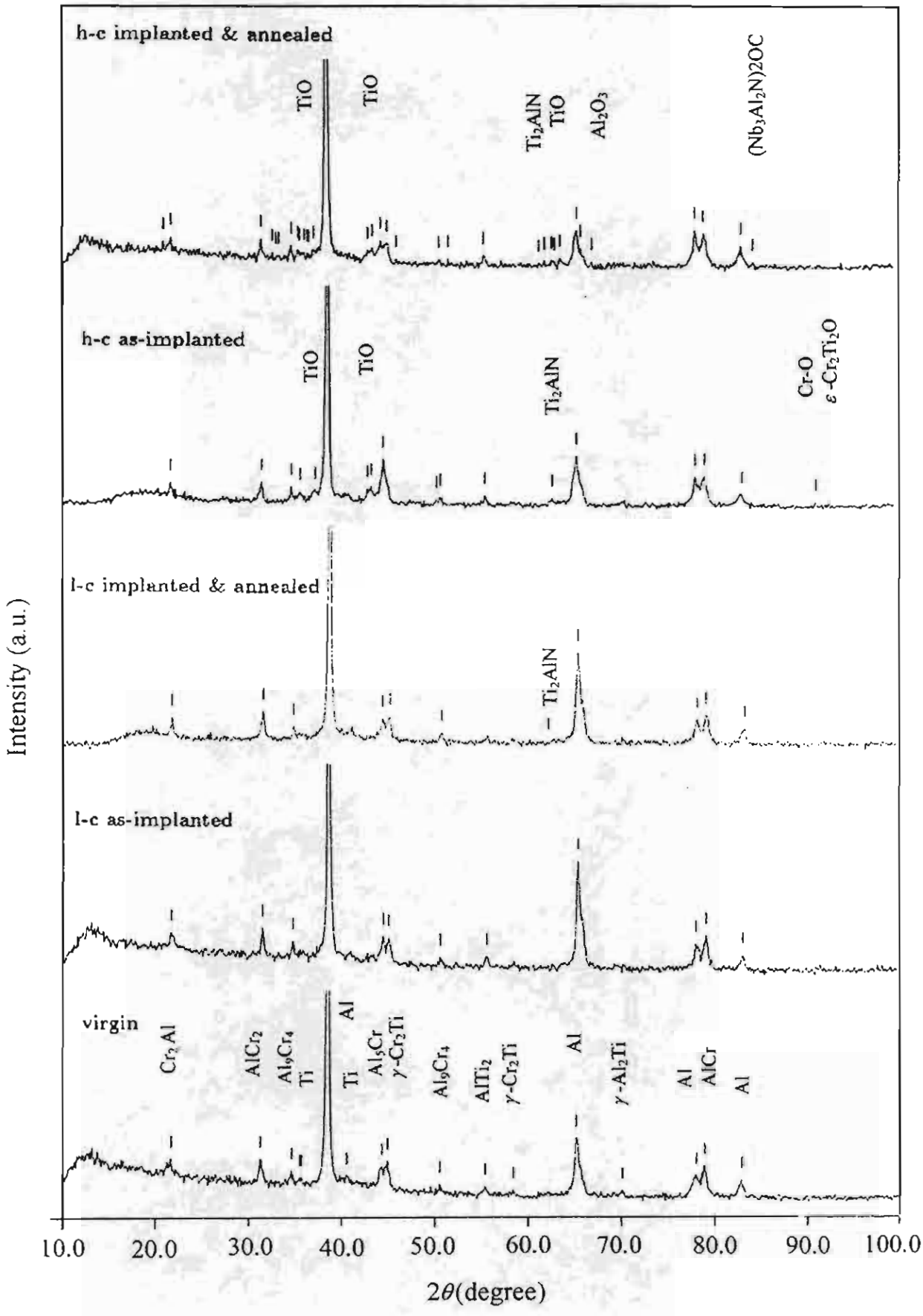
h-c implanted & annealed
TiO
TiO
Ti2AlN
TiO
Al2O3
(Nb3Al2N)2OC
h-c as-implanted
TiO
TiO
Ti2AlN
Cr-O
ε-Cr2Ti2O
l-c implanted & annealed
Ti2AlN
l-c as-implanted
virgin
Cr2Al
AlCr2
Al9Cr4
Ti
Al
Ti
Al5Cr
γ-Cr2Ti
Al9Cr4
AlTi2
γ-Cr2Ti
Al
γ-Al2Ti
Al
AlCr
Al
Intensity (a.u.)
10.0
20.0
30.0
40.0
50.0
60.0
70.0
80.0
90.0
100.0
2θ(degree)

Fig. 3

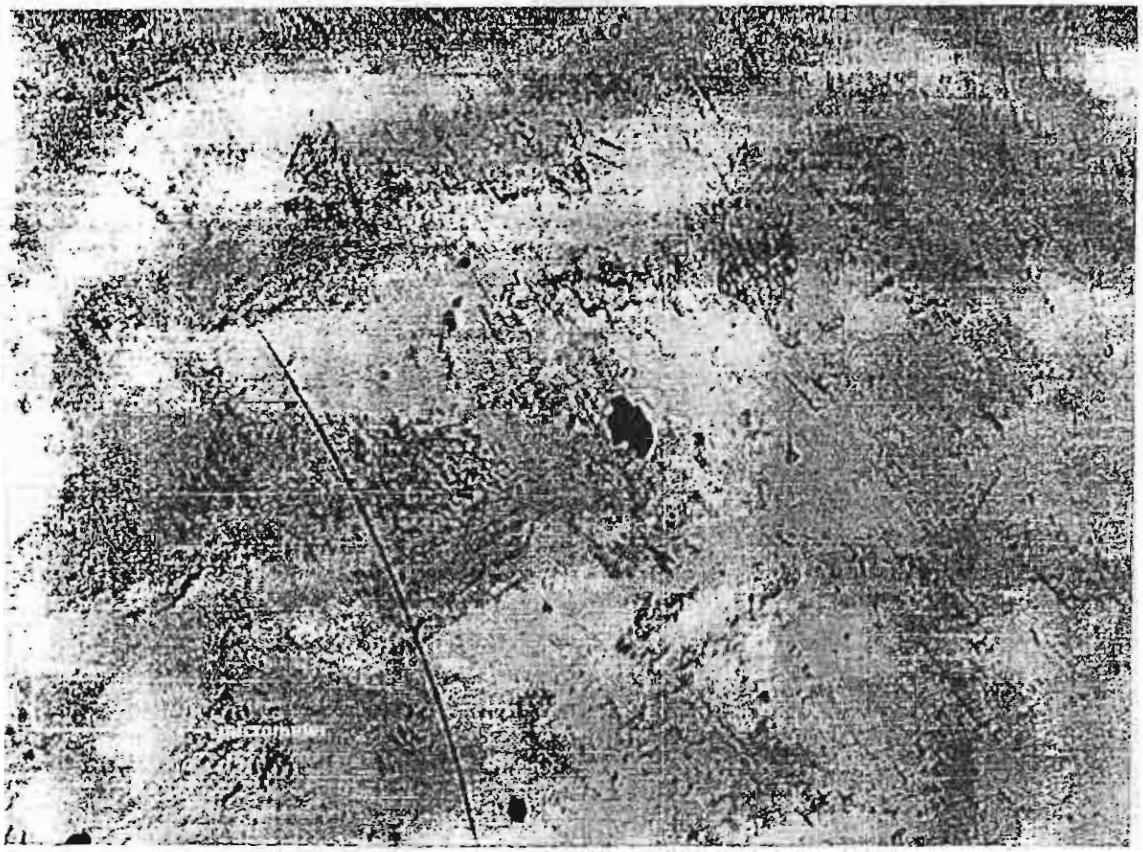

Fig. 4 (a)

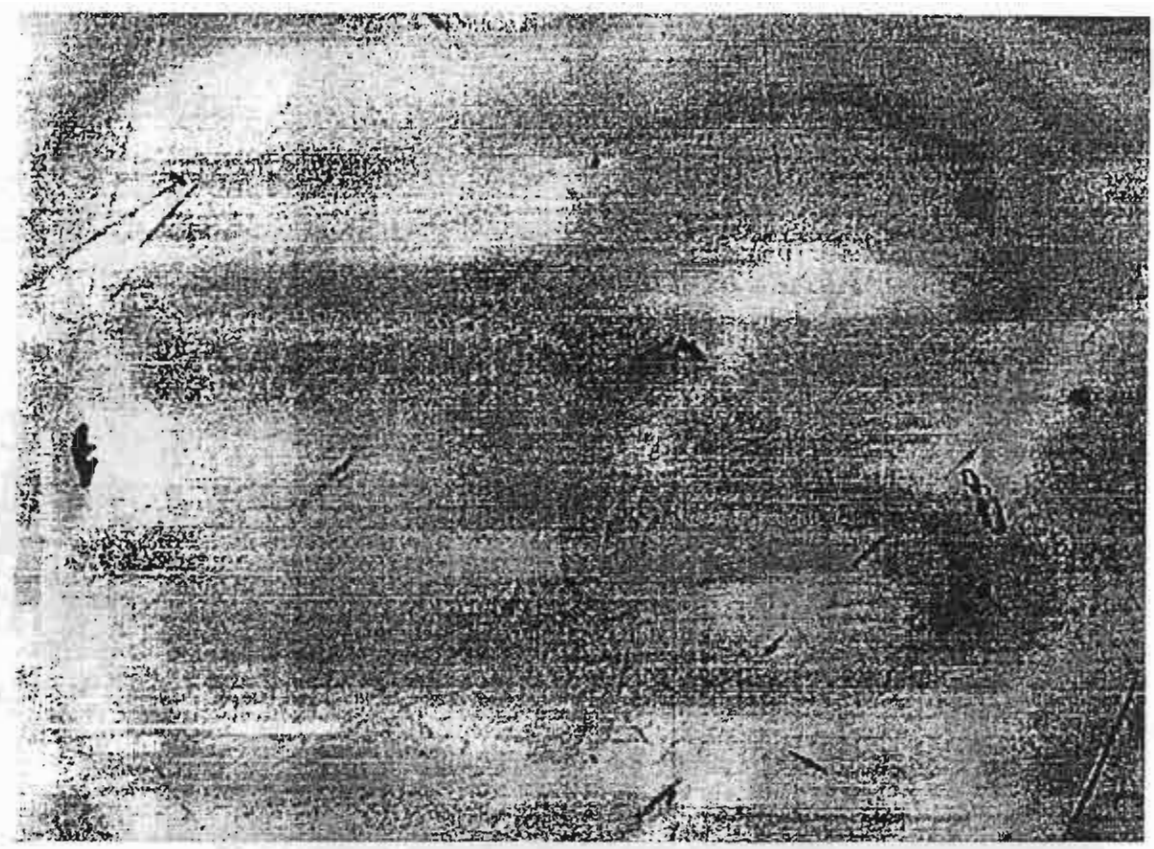

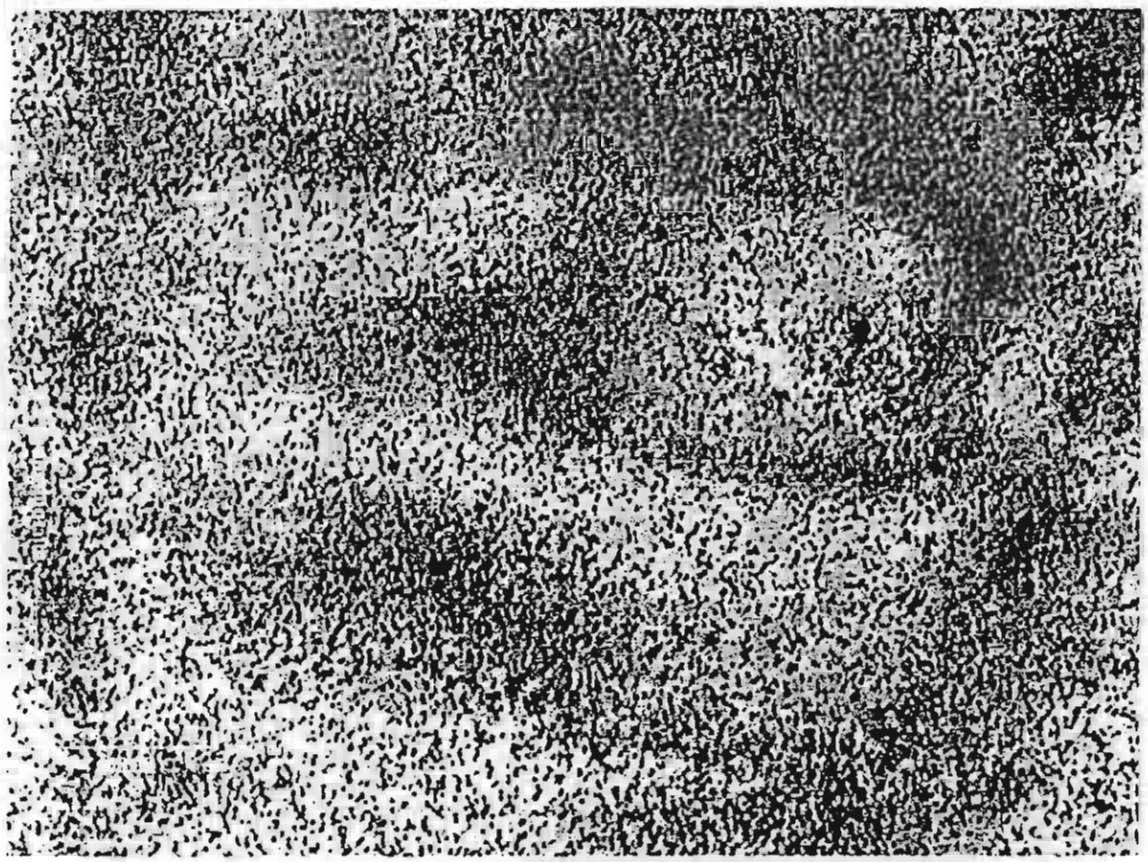

Fig. 4 (b)

(a)

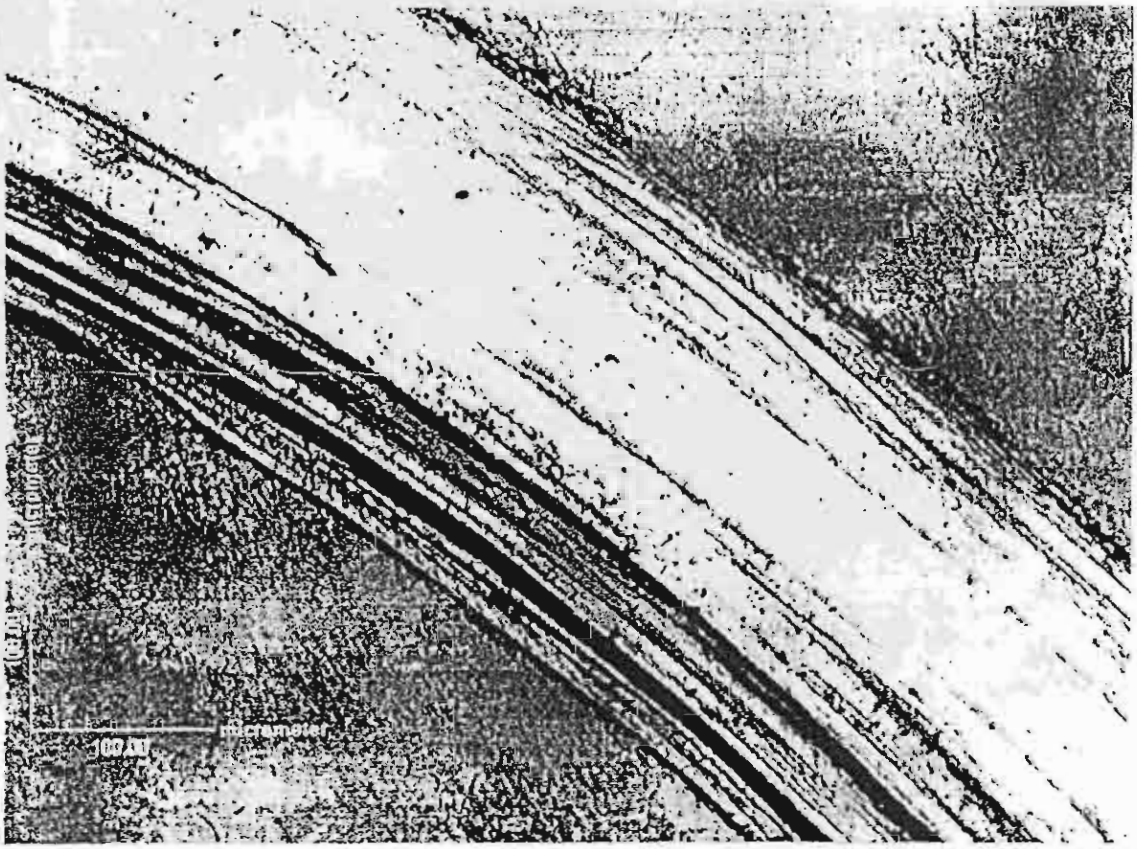

(b)

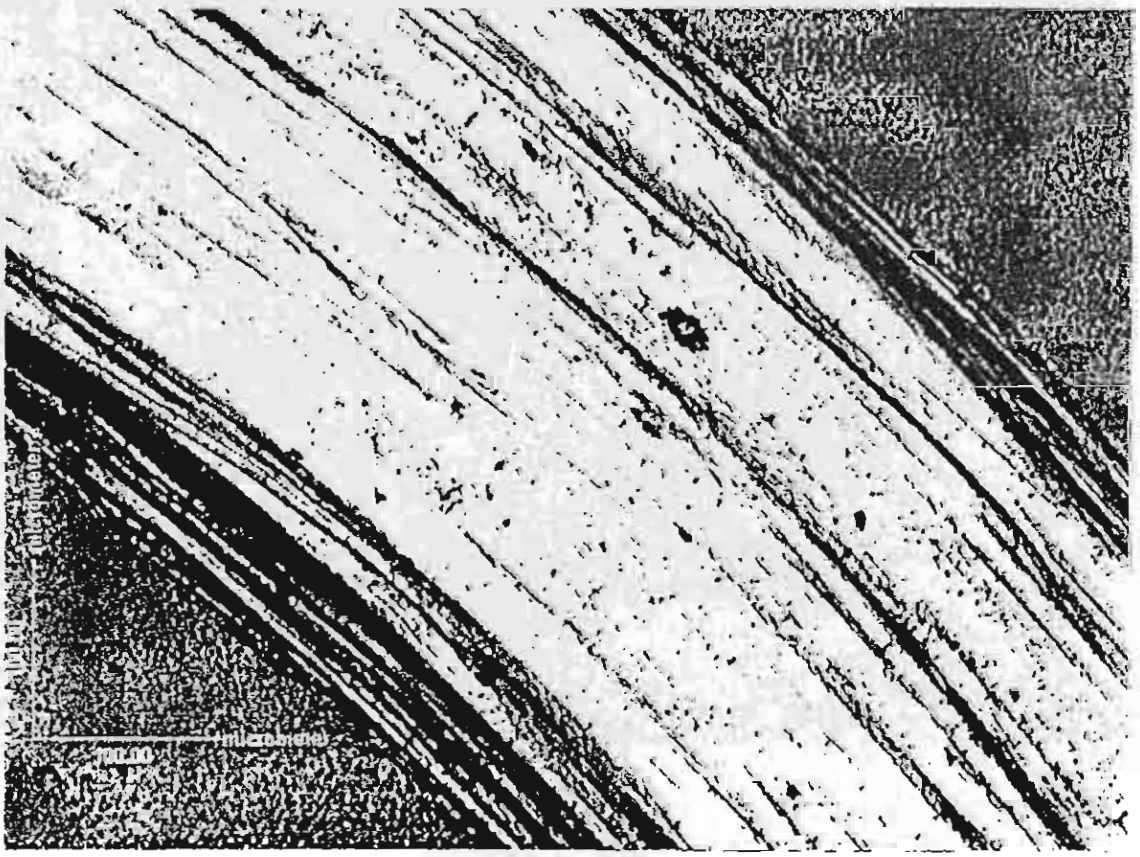

Fig. 5

# ภาคผนวก ข.

# Compact Multiparameter Thermoluminescence Spectrometer

Introducing a new generation high resolution, high performance TL reader for use in Thermoluminescence Dosimetry, material dating, and other applications where low level thermoluminescent samples are used. This new class of TL reader goes beyond simple integrated intensity responses over wavelength and allows you to separate individual spectrums.

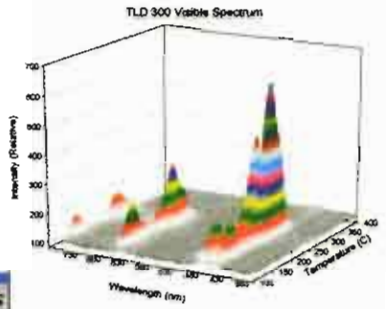


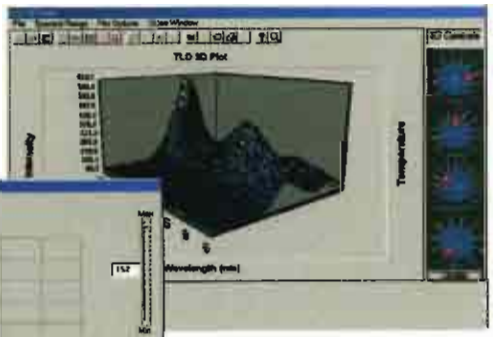


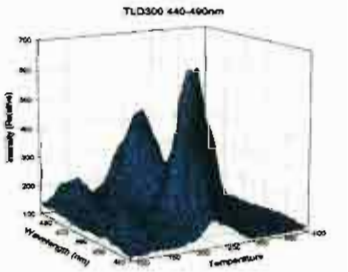


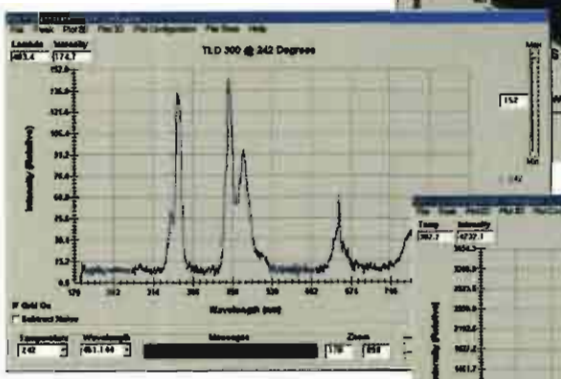


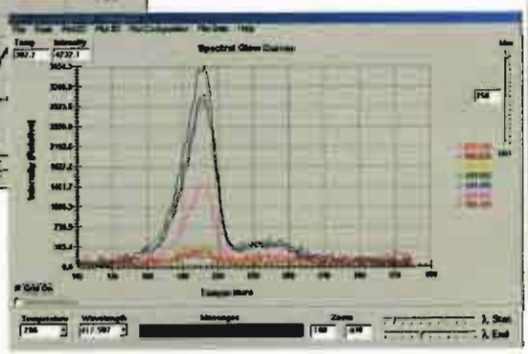

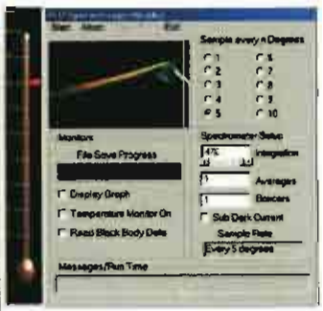

## Features

- *Simple Operation*
- *Adjustable Sensitivity (integration period)*
- *Black Body noise compensation*
- *Real Time display of temperature*
- *Fiber optic coupled to sample eliminating need for cooling detector and reduces electrical noise*
- *Built in 2D/3D plotting and analysis*
- *Save data for import into Excel, SigmaPlot or other programs for further analysis*
- *Print plots to any printer or save as image file for importing into word processing software*
- *Spectrum breakdown to any preset range or user defineable range*
- *Glow curve plots to simulate PMT responses of conventional TL Readers*

## System Specificatons

- *1.2 nm Wavelength Resolution*
- *Range from 200 to 850 nm*
- *Temperature Accuracy 1°C*
- *TL Sample Heating Range 25 - 500°C*
- *Precision Heater Timing 0.25%*
- *Sensitivity 5Gy $CaF_2$:Tm*

## System Requirements

- *Windows 95/98/NT*
- *Pentium 233MHz*
- *32Mbyte Ram*
- *10 Mbyte Installation Disk Space*

The Thailand Research Fund
539/2 Sri-Ayudhyai Rd.
Bangkok, 10400
Tel: (02) 6425186-9 Ext. 120

**Contact for more information and price**

Fast Neutron Research Facility
Chiangmai University
Chiangmai, 50200
Tel. (053) 943379, 942464